

## Floquet spin and spin-orbital Hamiltonians and doublon-holon generations in periodically driven Mott insulators

Kasra Hejazi,<sup>1</sup> Jianpeng Liu,<sup>2</sup> and Leon Balents<sup>2</sup>

<sup>1</sup>*Department of Physics, University of California, Santa Barbara, California 93106, USA*

<sup>2</sup>*Kavli Institute for Theoretical Physics, University of California, Santa Barbara, California 93106, USA*



(Received 25 September 2018; revised manuscript received 20 April 2019; published 9 May 2019)

We consider Mott insulators driven by periodic coherent laser radiation, using both single-orbital and multiorbital models, noting that the latter is of more interest in solid-state systems. We derive general expressions for the resulting periodically driven spin models and spin-orbital models using time-dependent perturbation theory. First, we show that the effective exchange interactions of the Floquet Hamiltonians are highly tunable by the frequency, amplitude, and polarization of the laser. Second, we take the effect of finite bandwidth of excitations into account and study possible heating effects. Using the same formalism with a slight modification we also consider the small-frequency regime and study the dielectric breakdown of Mott insulators.

DOI: [10.1103/PhysRevB.99.205111](https://doi.org/10.1103/PhysRevB.99.205111)

### I. INTRODUCTION

The study of periodically driven quantum systems has received significant attention in recent years. A common theoretical prescription is the Floquet formalism [1,2], which amounts to finding the eigenstates of the time evolution operator  $U(T+t, t)$  from time  $t$  to  $t+T$ , where  $T$  is the period of the drive. These states have the form  $e^{-i\epsilon_n t} |n\rangle_t$ , with  $|n\rangle_t$  a periodic state with the same period as that of the drive and  $\epsilon_n$  called the quasienergy. This form for eigenstates ultimately allows for a description of a time-periodic system using some time-independent Hamiltonian dubbed as the “Floquet Hamiltonian,”  $H_F = i\hbar \log U(T, 0)/T$ , where  $U(T, 0)$  is the stroboscopic time-evolution operator from time 0 to a full period  $T$ . One can further write down the evolution operator from arbitrary time  $t_0$  to another arbitrary time  $t$  with the use of the operators called the micromotion operators, as  $U(t, t_0) = \hat{U}_F(t) e^{-iH^{\text{eff}}(t-t_0)} \hat{U}_F^\dagger(t_0)$ , where  $H^{\text{eff}}$  is a time-independent effective Hamiltonian and  $\hat{U}_F(t)$ , the micromotion operator, is a periodic operator yielding intraperiod dynamics [3,4].

A natural way to periodically drive a condensed matter system is with electromagnetic radiation. Since the details of the Floquet Hamiltonian describing this situation are crucially dependent on the frequency, amplitude, and polarization of the external drive, one is able to engineer the physical properties of a quantum system to a large extent using laser-light radiation [5]. Such “Floquet engineering” has been extensively studied in the context of both single-particle and many-body condensed-matter physics. In noninteracting systems, the light radiation dresses the electronic band structure, which may change the topological character, leading to various exotic phenomena [6–16]. On the other hand, in interacting systems the Floquet physics has been explored in the context of the light-induced/light-enhanced superconducting [17–21], charge-density-wave [22], and spin-density-wave [23] Fermi-surface instabilities. Laser-controlled exchange interactions in single-band Mott insulators [24], topological phase transitions in Kondo insulators [25], and the possible periodically

driven topologically ordered states [26,27] have also been discussed. There are also many papers exploring Floquet engineering in bosonic Hubbard models based on the high-frequency Floquet-Magnus expansion which assumes the drive frequency  $\omega$  is much larger than the hopping  $t$  [28–30]. In that regime, an effective bosonic Hubbard model can be derived with occupation-dependent hopping, amenable to more standard analysis. This approach is complimentary to the one we will adopt below, in which we focus on fermions (i.e., electrons) and keep the frequency of the same order as the Hubbard repulsion but assume that the hopping is small compared to the Hubbard repulsion and that the particle density is close to single-occupancy, which is the criterion for the Mott state.

In the presence of interactions, one expects a periodically driven system to eventually heat up to infinite temperature at long times [31,32], i.e., that the density operator of any finite subsystem become maximally mixed and featureless at long times. However, as has been shown rigorously, the heating rate can be (quasi-)exponentially slow [33–35] in the ratio of the driving frequency to the local energy scales. As a result of this, one expects such system to show interesting prethermal behavior. One can even think of the possibility for a system to first relax into a steady prethermal state at intermediate times  $t \lesssim \tau^*$ , then ultimately evolve into the infinite-temperature state at long times  $t \gtrsim \tau^*$ . Such a prethermal regime is realized numerically in Ref. [36], where it has been shown in a lattice spin model that such a system can first equilibrate to a (pre)thermal state with respect to a time-independent effective Hamiltonian before it reaches the infinite-temperature state. Such time-independent effective Hamiltonians are dubbed “Floquet Hamiltonians” in the literature and are typically expressed as series expansions in  $1/\omega$ . Furthermore, it has been explicitly shown in Ref. [36], using numerics, that the characteristic infinite-temperature timescales  $\tau^*$  in their models grow exponentially with the increase of the driving frequency.

We will study periodically driven Mott insulators in this work. We start with single-orbital Mott insulators, i.e., the

Hubbard model, at half filling. The effective spin Floquet Hamiltonian for periodically driven half-filled Hubbard model has been derived [24,26,37]. In the static case, in an insulator, the Hubbard model has two relevant energy scales: (i) the energy scale of spin dynamics, i.e., exchange interaction  $J$  between the electrons at neighboring sites, and (ii) the onsite electron-electron interaction energy  $U$ , which comes into play when there are doubly occupied sites. In the Mott-insulating regime, the latter is much larger than the former,  $U \gg J$ . The periodically driven Hubbard model, on the other hand, has another energy scale that is the driving frequency  $\omega$ . Following similar arguments as in the previous paragraph, one should be concerned about the regime in which a rapid heating does not occur in this system. There are two classes of processes that can lead to heating of the system due to the absorption of photons: one is by multispin reorderings, and the other is by creation of doubly occupied sites in the system. Considering the second case, one can think of the doubly occupied sites (doublons) and the empty sites (holons) which are created as a consequence as new dynamical degrees of freedom. Due to the hopping of electrons in the original Hubbard model, the doublons and the holons are able to hop around and thus these excitations of the system have a nonvanishing bandwidth [38,39]. If photons that strike the system are able to supply an energy that lies within this bandwidth, one expects to see a rapid heating due to creation of doublon-holon (DH) pairs in the system. As we will see, heating can be avoided if the frequency is kept outside of certain resonant windows and, at the same time, also kept much larger than the effective spin exchange. In this paper, we will restrict our attention to states with very low density of DH pairs and will develop a time-dependent perturbation theory that will take the above points into account.

Most of the previous theoretical studies of similar Floquet systems have been focused on spin degrees of freedom and the electron-phonon couplings. To the best of our knowledge, the orbital degrees of freedom and their interplay with the spins have never been addressed in the context of Floquet physics. This is most relevant to solid-state Mott insulators like titanates, nickelates, and manganites. Given that the orbitals play essential roles in strongly correlated transition-metal oxides [40–42], in this paper we next consider driving multiorbital Mott insulators using laser radiation. We use multiorbital Hubbard models to describe such systems, with the on-site electron interactions much greater than the hopping parameters, and we consider the filling equal to one electron per site. In a multiorbital Mott insulator, the on-site interaction energy depends on the spin and orbital configurations of the electrons at a multiply occupied site. Furthermore, for a hopping event between two given sites, the hopping parameters can also depend on the initial and final orbital configurations of the sites. This added complexity of multiorbital Mott insulators has an upside: It introduces more freedom to engineer the exchange interactions in the effective Floquet Hamiltonian.

Based on time-dependent perturbation theory, we first derive general expressions for the time evolution in the periodically driven spin and spin-orbital models. Including the effects of the DH hoppings, i.e., taking the effect of the bandwidth of excitations into account in our perturbation theory, we find

that the Floquet Hamiltonian projected onto a generic state in the zero-doublon subspace contains both real and imaginary parts. The real part is interpreted as an effective spin or spin-orbital model, and the corresponding exchange interactions are renormalized by the periodic driving, which allows for the Floquet engineering of the interactions. The imaginary part, on the other hand, is related to the rate of generation of DH pairs and thus can capture the effects of heating, due to the increase in the density of DH pairs. This said, one can work in two different regimes using the formalism of this paper. Either one is away from a resonance and not too many DH pairs are created, and thus a spin(-orbital) effective Hamiltonian captures the physics well, or one is inside one of the resonant windows and the physics of the system, at least for a short time, is described by studying how DH pairs density increases as a result of resonant radiation. We furthermore study, by slightly altering the formalism, the creation rate of DH pairs at very small frequencies and show that indeed a nontrivial zero-frequency limit exists. The results in this limit can be interpreted as the behavior of the system when exposed to static external field, and thus is a reflection of the (static) field-induced breakdown of a Mott insulator.

In a prior short paper [43], some parts of this formalism were presented and applied to the orthorhombic titanates  $\text{YTiO}_3$  and  $\text{LaTiO}_3$  using first-principles calculations. It was observed that as a result of multiorbital interactions, ferromagnetic and antiferromagnetic Mott insulators exhibit distinct responses to laser radiation. The effective exchange interactions in these titanates may be engineered to a large extent and may be even flipped at moderate electric-field energies. The present paper derives and extends the formalism of this earlier work and discusses in much more detail the physics of doublon generation.

The remainder of this paper is organized as follows. In Sec. II we discuss the formalism of the Floquet spin model derived from the periodically driven Hubbard model and apply it to a single-orbital Hubbard model. In Sec. III we generalize the formalism to the case of multiorbital Mott insulators. We finally present a summary of what has been done in the paper.

## II. FLOQUET SPIN MODEL

We start the discussion with a half-filled single-orbital Hubbard model which is periodically driven by laser radiation. Such a problem has been discussed in Refs. [24,26,37]. Here we rederive the effective Floquet spin Hamiltonian using time-dependent perturbation theory and show that one can capture novel physics if one takes the effect of the finite bandwidth of the excitations into account. We later will use similar methods to generalize the discussions to multiorbital Mott insulators.

### A. Time-dependent perturbation theory

We consider the following periodically driven Hubbard model:

$$H(t) = - \sum_{\langle ij \rangle \sigma} (t_h e^{i u_{ij} \sin \omega t} c_{i\sigma}^\dagger c_{j\sigma} + \text{H.c.}) + U \sum_i \hat{n}_{i\uparrow} \hat{n}_{i\downarrow}, \quad (1)$$

where  $t_h$  is the hopping amplitude between sites  $i$  and  $j$  and  $U \gg t_h$  is the onsite Coulomb repulsion energy;  $u_{ij} = e\mathbf{E}_0 \cdot \mathbf{r}_{ij}/\omega$  (we have set  $\hbar = 1$ ), where  $|\mathbf{E}_0|$  denotes the magnitude of the oscillating electric field of a laser with frequency  $\omega$ ,  $\mathbf{E}(t) = \mathbf{E}_0 \cos \omega t$ ; and  $\mathbf{r}_{ij}$  is the displacement vector between two lattice sites  $i$  and  $j$ . Only the nearest-neighbor hopping is taken into account here and the model is studied at half-filling. Note that Hermiticity requires  $u_{ij} = -u_{ji}$ .

In equilibrium without driving it is well known that at half filling the system stays in the Mott-insulating phase in the limit  $U \gg t_h$ . Then the low-energy physics is dominated by the spin dynamics and is well described by a Heisenberg model with antiferromagnetic nearest-neighbor exchange,  $J_{ij} = 4t_h^2/U$ ; this result can be derived using a second-order time-independent perturbation theory [44]. We generalize the discussions to the case with periodic laser radiation and derive a *time-dependent* spin model using time-dependent second-order perturbation theory.

A generic many-body state  $|\Psi\rangle_t$  can be expressed as a linear superposition of states with  $n$  doubly occupied sites (which are dubbed as ‘‘doublons’’):  $|\Psi\rangle_t = \sum_{n=0}^{\infty} |\Psi_n\rangle_t$ , where  $|\Psi_n\rangle_t$  represents the component of the state of the system with  $n$  doublons, i.e.,  $U \sum_i \hat{n}_{i\uparrow} \hat{n}_{i\downarrow} |\Psi_n\rangle_t = nU |\Psi_n\rangle_t$ . The Schrödinger equation for the evolution of the different components of the state of the system reads:

$$\begin{aligned} i\partial_t |\Psi_0\rangle_t &= \hat{P}_0 H |\Psi\rangle_t = \hat{P}_0 T_t |\Psi_1\rangle_t, \\ i\partial_t |\Psi_1\rangle_t &= \hat{P}_1 H |\Psi\rangle_t = U |\Psi_1\rangle_t + T_t |\Psi_0\rangle_t \\ &\quad + \hat{P}_1 T_t |\Psi_1\rangle_t + \hat{P}_1 T_t |\Psi_2\rangle_t, \\ &\vdots \end{aligned} \quad (2)$$

where  $T_t = -\sum_{(ij)\sigma} (t_h e^{iu_{ij} \sin \omega t} c_{i\sigma}^\dagger c_{j\sigma} + \text{H.c.})$  is the time-dependent hopping term in the Hamiltonian (1) and  $\hat{P}_n$  is the projector onto the subspace with  $n$  double occupancies.

Since we are interested in the dynamics of states with a small local density of doublons and holons, we approximately consider only the dynamics induced by  $|\Psi_1\rangle_t$  for the component  $|\Psi_0\rangle_t$  and neglect corrections due to the effects of  $|\Psi_n\rangle_t$ , with  $n > 1$ . We claim that the essential properties of the dynamics of the system can be captured by this approximation. Thus we will continue by neglecting the  $\hat{P}_2|\Psi\rangle$ ,  $\hat{P}_3|\Psi\rangle$ , ... components of the time-dependent state in the above Schrödinger equation and focusing on how  $|\Psi_0\rangle$  and  $|\Psi_1\rangle$  evolve mutually. Note that these higher-order components will contribute with at least the fourth order of  $t_h$  to the time evolution of the spin state. The truncated equations of motion take the following form:

$$\begin{aligned} i\partial_t |\Psi_0\rangle_t &= \hat{P}_0 T_t |\Psi_1\rangle_t, \\ i\partial_t |\Psi_1\rangle_t &= U |\Psi_1\rangle_t + T_t |\Psi_0\rangle_t + \hat{P}_1 T_t |\Psi_1\rangle_t. \end{aligned} \quad (3)$$

The hopping operator  $P_1 T_t$  in the second line of (3) can be replaced by  $\tilde{T}_t = P_1 T_t P_1$  since it is acting on the one double-occupancy subspace. One can think of the action of the operator  $\tilde{T}_t$  as the hopping operator of the doublon and holon restricted to the 1 DH pair subspace. Note that we have kept the term  $T_t |\Psi_1\rangle_t$  in the above equation, although it will give the same order corrections to the dynamics of  $|\Psi_0\rangle_t$  as the terms that are neglected. The reason is that it accounts for the

effects of the finite bandwidth of excitations, which can give rise to a form of heating due to the creation of doublon-holon pairs. We will discuss these matters more in what follows.

We will restrict our attention for now to the regime in which the frequency is much larger than the hopping amplitude  $t_h$ ; one continues with (3) by approximating the hopping operator within the single DH subspace  $\tilde{T}_t$  by its time average (Appendix A),

$$\begin{aligned} \bar{T} &= \frac{\omega}{2\pi} \int_0^{2\pi/\omega} dt' \tilde{T}_{t'}, \\ &= t_h \sum_{\langle ij \rangle} \{ [\mathcal{J}_0(u_{ij}) \hat{P}_1 \hat{v}_{ij} \hat{P}_1] + (i \leftrightarrow j) \}, \end{aligned} \quad (4)$$

where  $\mathcal{J}_n$  stands for the Bessel function of the first kind and  $\hat{v}_{ij} = (-\sum_\sigma c_{i\sigma}^\dagger c_{j\sigma})$  is the hopping operator for the electrons. The operator  $\hat{P}_1 \hat{v}_{ij} \hat{P}_1$  is the hopping operator for the doublon and the holon. The second equation of (3) reads thus:

$$e^{-i(U+\bar{T})t} i \partial_t [e^{i(U+\bar{T})t} |\Psi_1\rangle_t] = T_t |\Psi_0\rangle_t. \quad (5)$$

Integrating both sides and fixing the initial conditions such that the lower limits of the integrals cancel each other, one arrives at:

$$\begin{aligned} i [e^{i(U+\bar{T})t} |\Psi_1\rangle_t] &= t_h \int^t dt' e^{i(U+\bar{T})t'} \sum_{\langle ij, n \rangle} \\ &\quad \times \{ [\mathcal{J}_{-n}(u_{ij}) e^{-in\omega t'} \hat{v}_{ij}] + (i \leftrightarrow j) \} |\Psi_0\rangle_{t'}. \end{aligned} \quad (6)$$

In the above equation we have used  $e^{iA \sin \omega t} = \sum_{n=-\infty}^{\infty} \mathcal{J}_n(A) e^{in\omega t}$ . Noting that  $|\Psi_0\rangle_t$  is a slow function of time, one can integrate by parts and drop the resulting integral, as being higher order in  $t_h$ :

$$\begin{aligned} |\Psi_1\rangle_t &= -t_h \left( \sum_{\langle ij, n \rangle} \left\{ \left[ \mathcal{J}_{-n}(u_{ij}) \frac{e^{-in\omega t}}{U - n\omega + \bar{T}} \hat{v}_{ij} |\Psi_0\rangle_t \right] \right. \right. \\ &\quad \left. \left. + (i \leftrightarrow j) \right\} + \mathcal{O}(t_h^2/U^2) \right). \end{aligned} \quad (7)$$

The remainder is  $\mathcal{O}(t_h^2/U^2)$ , because it comes from neglecting an integral which contains a factor of  $1/(U - n\omega)$  and a time derivative of  $|\Psi_0\rangle_t$ , which has leading-order contribution proportional to  $t_h/U^2$ , as we will see. Note also that we are collectively showing all  $U - n\omega$  by  $U$  in the argument of  $\mathcal{O}$ . One can plug this back into the first equation of (3) to get the following relation for the time evolution equation of  $|\Psi_0\rangle_t$ :

$$\begin{aligned} i\partial_t |\Psi_0\rangle_t &= \sum_{\langle ij, (i'j'), mn \rangle} \{ [f_{i'j'ij}^{mn}(t) \hat{G}_{i'j'ij}(U - n\omega) |\Psi_0\rangle_t] \\ &\quad + (i \leftrightarrow j) \} + [i' \leftrightarrow j'], \end{aligned} \quad (8)$$

where

$$f_{i'j'ij}^{mn}(t) = -e^{i(m-n)\omega t} \mathcal{J}_{-n}(u_{ij}) \mathcal{J}_m(u_{i'j'}), \quad (9)$$

and the operator

$$\hat{G}_{i'j'ij}(E) = t_h^2 \hat{P}_0 \hat{v}_{i'j'} \frac{1}{E + \bar{T}} \hat{v}_{ij} \hat{P}_0, \quad (10)$$

creates a DH pair at  $(i, j)$ , propagates it according to  $(E + \bar{T})^{-1}$ , and, finally, annihilates the pair at  $(j', i')$ .

Let us first consider a situation where  $U - n\omega \gg t_h$  in Eq. (8), under this condition one is able to neglect  $\bar{T}$  in the operator  $\frac{1}{U - n\omega - \bar{T}}$  which appears in  $G(U - n\omega)$  and thus  $G(U - n\omega)$  can be well approximated by  $t_h^2 [P_0 \hat{v}_{i'j'} \frac{1}{U - n\omega} \hat{v}_{ij} P_0]$ . Noting that the fraction  $\frac{1}{U - n\omega}$  is a number and that  $P_0 \hat{v}_{ji} \hat{v}_{ij} P_0 = (\frac{1}{2} - 2 \mathbf{S}_i \cdot \mathbf{S}_j) P_0$ , the evolution equation for  $|\Psi_0\rangle_t$  becomes

$$i \partial_t |\Psi_0\rangle_t = - \sum_{(ij)} J_{ij}(t) \left( \frac{1}{4} - \mathbf{S}_i \cdot \mathbf{S}_j \right) |\Psi_0\rangle_t, \quad (11)$$

with

$$J_{ij}(t) = \sum_{m,n=-\infty}^{\infty} e^{i(m-n)\omega t} \mathcal{J}_m(u_{ji}) \mathcal{J}_n(u_{ji}) \left( \frac{4t_h^2}{U - n\omega} \right).$$

Since  $J_{ij}(t)$  is periodic, the above equation of motion can be treated using the Floquet formalism. By virtue of a high-frequency expansion, the Floquet effective Hamiltonian can be expanded in a power series in  $1/\omega$ ,  $H^{\text{eff}} = \sum_{n=0}^{\infty} H_n/\omega^n$ , where  $H_n$  is  $\mathcal{O}(J_{ij}^{n+1})$ . When the driving frequency  $\omega$  is much larger than the exchange energy, the leading term is given by time averaging [3,4]:

$$H^{\text{eff}} = \frac{\omega}{2\pi} \int_0^{2\pi/\omega} dt \left[ \sum_{(ij)} J_{ij}(t) \mathbf{S}_i \cdot \mathbf{S}_j \right] + \mathcal{O}(J_{ij}^2/\omega). \quad (12)$$

Here we have dropped the constant term. With time averaging one arrives at the effective exchange parameter:

$$\bar{J}_{ij} = \frac{\omega}{2\pi} \int_0^{2\pi/\omega} dt J_{ij}(t) = \sum_{n=-\infty}^{\infty} \frac{4t_h^2 \mathcal{J}_n^2(u_{ij})}{U - n\omega}. \quad (13)$$

This shows that the effective spin exchange interaction of the Floquet spin Hamiltonian associated with the bond  $ij$  is renormalized due to the periodic driving and becomes dependent on both the frequency and amplitude of the drive,  $J_{(ij)} = \sum_{n=-\infty}^{\infty} 4t_h^2 \mathcal{J}_n^2(u_{ij}) / (U - n\omega)$ . Moreover, the summation over  $n$  shows the contribution of all the virtual DH excitation processes which absorb/emit integer numbers of photons, and each  $n$ -photon process is weighted by  $\mathcal{J}_n^2(u_{ij})$ . The energy of the virtually created DH pair which absorbs/emits  $n$  photons is just  $U - n\omega$  because the effects of DH hoppings are neglected. Note that this is a reproduction of the results reported in previous studies [24,26,37].

One expects the above result to be valid up to large times [34], i.e., (quasi-)exponential in the ratio of frequency to effective exchange energy scale,  $t_h^2/U$ , and not after that due to Floquet thermalization of the system; the system becomes featureless and locally indistinguishable from an infinite-temperature system, due to the absorption of energy in the form of reorderings in the spin configuration of the system.

However, the system would also be heated up by absorbing photons to create doublon-holon pairs. When the rate of DH generations is non-negligible, the local properties of the system can no longer be captured by the low-energy spin dynamics.

The result in Eq. (13) shows no imaginary part for the effective exchange interaction, and hence the effective Floquet

Hamiltonian dynamics in the 0-doublon subspace shows no departure from this subspace; thus the physics of doublon-holon creation is not captured by this result. The reason for this is that the finite bandwidth of the virtual doublon-holon pairs in the time-dependent perturbation theory is neglected by dropping  $\bar{T}$  in the definition of  $G$  [Eq. (10)]. We will study the effects that arise from restoring the finite bandwidth of these excitations next.

With the above considerations in mind, one can think of expanding  $G$  in Eq. (10) in a power series as follows:

$$G_{i'j'ij}(E) = P_0 v_{i'j'} \left\{ \frac{1}{E} \left[ 1 + \left( -\frac{\bar{T}}{E} \right) + \left( -\frac{\bar{T}}{E} \right)^2 + \left( -\frac{\bar{T}}{E} \right)^3 + \dots \right] \right\} v_{ij} P_0. \quad (14)$$

The above series indicates that one should take into account all the possible virtual hopping processes taking place for the virtual doublon-holon pair. The effect of considering all virtual hopping processes is twofold. First, it introduces sub-leading corrections to the evolution equation for  $|\Psi_0\rangle_t$  [analog of (11)]—these corrections can be of the same Heisenberg-interaction form as in (11) and may include new forms like four-spin interactions. Note that we have already dropped comparable corrections by working up to the second order in our time-dependent perturbation theory. Second, and most important for our purposes, they account for the effects of a finite bandwidth of the virtual excitations involved. To treat this in what follows we make a key assumption: We only consider the hopping processes which bring the DH pairs back to where they were created, with a final spin configuration which is identical to the initial configuration. Taking the other *nonlocal* processes into account will bring in higher-order effects in the interaction terms and also the bandwidth of excitations. With the above assumption, it follows that

$$i \partial_t |\Psi_0\rangle_t = \sum_{(ij)} \sum_{m,n=-\infty}^{\infty} [H_{ij}^{mn}(t) |\Psi_0\rangle_t] + (i \leftrightarrow j), \quad (15)$$

where

$$H_{ij}^{mn}(t) = \sum_{\sigma\sigma'} t_h^2 f_{ij}^{mn}(t) c_{j\sigma'}^\dagger c_{i\sigma}^\dagger c_{i\sigma} c_{j\sigma} g_{\text{dh}}(U - n\omega), \quad (16)$$

$g_{\text{dh}}(E) = {}_t \langle \Psi_0 | c_{j\sigma}^\dagger c_{i\sigma} (E + \bar{T})^{-1} c_{i\sigma}^\dagger c_{j\sigma} | \Psi_0 \rangle_t$  is the DH Green's function, and  $f_{ij}^{mn}(t)$  is defined in Eq. (9). Note that the dependence of  $g_{\text{dh}}$  on  $(i, j, \sigma, \sigma')$  and also the state  $|\Psi_0\rangle_t$  is understood despite the notation not showing it.

## B. The Green's function

To calculate the Green's function of the virtual doublon-holon pair, we decompose the time-averaged DH pair hopping operator  $\bar{T}$  into a sum of a doublon-hopping and a holon-hopping term,  $\bar{T} = \bar{T}_d + \bar{T}_h$ , with  $\bar{T}_d$  and  $\bar{T}_h$  the hopping operator for the doublon and the holon in the 1-doublon subspace. In principle, the motions induced by  $\bar{T}$  (which is the time-averaged hopping restricted to the 1-doublon subspace), for the doublons and for the holons are correlated, but following Ref. [45], we neglect the correlations between the motions of



the doublons and the holons. We also add an infinitesimal negative imaginary part to the denominator of the Green's function which can be interpreted as the reciprocal of the time over which the drive is turned on,

$$\begin{aligned} g_{\text{dh}}(E - i\delta) &= \langle \Psi_0 | c_{j\sigma}^\dagger c_{i\sigma} \left( \frac{1}{E + \bar{T} - i\delta} \right) c_{i\sigma}^\dagger c_{j\sigma} | \Psi_0 \rangle \\ &= -i \int \frac{d\Omega}{2\pi} \langle \Psi_0 | c_{j\sigma}^\dagger c_{i\sigma} \frac{1}{\Omega + \bar{T}_h - i\delta} \\ &\quad \times \frac{1}{E - \Omega + \bar{T}_d - i\delta} c_{i\sigma}^\dagger c_{j\sigma} | \Psi_0 \rangle \\ &= -i \int \frac{d\Omega}{2\pi} g_h(\Omega - i\delta) g_d(E - \Omega - i\delta), \end{aligned} \quad (17)$$

where  $g_d$  and  $g_h$  are the doublon and the holon Green's functions:

$$\begin{aligned} g_h(E - i\delta) &= \langle \Psi_0 | c_{j\sigma}^\dagger \frac{1}{E + \bar{T}_h - i\delta} c_{j\sigma} | \Psi_0 \rangle, \\ g_d(E - i\delta) &= \langle \Psi_0 | c_{i\sigma} \frac{1}{E + \bar{T}_d - i\delta} c_{i\sigma}^\dagger | \Psi_0 \rangle. \end{aligned} \quad (18)$$

Let us emphasize once more that in order to obtain the result of Eq. (17), we have assumed a mean-field approximation to be valid and that the motion of the doublon and that of the holon are not correlated [45].

To calculate the Green's functions defined above, we work in the retraceable path (RP) approximation proposed by Brinkman and Rice [38]. To compute the Green's function for a holon, for example, with the same initial and final locations and spin configurations [as in (18)], one needs to consider all the hopping processes which bring the particle back to its original location and in the meanwhile bring the spin configuration back to the original one; in the RP approximation scheme, this can be done if one takes every path that starts at the given location and terminates at the same point, with the constraint that the hopping holon should exactly retrace its forward-going path in its way back to the original location. With this constraint, every spin reordering that is done in the forward-going path is corrected when the particle is getting back to its original position. Note that this prescription does not capture all the possible processes; what is missing is the contribution by the paths that are closed loops and keep the final and initial spin configurations the same. As Brinkman and Rice showed, such closed loops will contribute first at order  $t_h^{12}$  in the antiferromagnetic spin background, for example, and are thus negligible. Note that the single doublon Green's function has the same analytical form as the holon Green's function.

Finally,  $g_{\text{dh}}$  for a generic state on the right-hand side of the first line of (15) can be approximated using the convolution integral in (17) in terms of  $g_h$  and  $g_d$ , which are calculated using an RP approximation. With this prescription, as we will see, the state dependence and also site dependence of the Green's functions  $g_h$ ,  $g_d$ , and therefore  $g_{\text{dh}}$ , when nonzero, are dropped. For a brief review of the RP approximation, we refer the reader to Appendix B.

As is shown in the Appendix, after Ref. [38], one has the following form for the holon Green's function in the RP

approximation:

$$g_h(E) = \frac{2(z-1)}{E[(z-2) + z\sqrt{1-4(z-1)\bar{t}_h^2/E^2}]}, \quad (19)$$

where  $z$  is the coordination number and  $\bar{t}_h = t_h \mathcal{J}_0(u_{ij})$  is the time-averaged hopping amplitude between sites  $i$  and  $j$ . Here we take the polarization of the radiation such that the electric field amplitude is isotropic and thus  $u_{ij}$  does not depend on the bond directions, for the sake of simplicity. However, in principle,  $u_{ij}$  is different for different bonds which makes the hopping  $\bar{t}_h$  anisotropic, and one needs to solve coupled self-energy equations for different bond directions self-consistently in order to calculate the holon's Green's function. A first approximation in that case will be to average the hopping amplitudes along the different bond directions. (Please refer to Appendix B for more discussion.) This kind of treatment is also adopted in the case of multiorbital Mott insulators as will be discussed in Sec. III.

It is obvious from the form in Eq. (19) that  $g_h(E)$  behaves as  $\frac{1}{E}$  for large values of  $E$ . Furthermore,  $g_h(E)$  when viewed in the complex  $\tilde{E} = E/(2\bar{t}_h\sqrt{z-1})$  plane has a branch cut with the two end points  $\tilde{E} = 1$  and  $\tilde{E} = -1$ . Note that  $g_d$  has the same analytic expression as  $g_h$ . With the above form of the Green's function for the doublon and the holon,  $g_{\text{dh}}$  is calculated as discussed in Appendix C. A plot of  $g_{\text{dh}}$  for  $z = 6$  obtained this way can be found in Fig. 1.

With  $g_{\text{dh}}$  at hand, it is easy to derive the effective exchange parameter, similarly to what was done previously:

$$\bar{J}_{ij} = \sum_{n=-\infty}^{\infty} 4t_h^2 \mathcal{J}_n^2(u_{ij}) g_{\text{dh}}(U - n\omega). \quad (20)$$

It can be seen from Fig. 1 that  $g_{\text{dh}}(U - n\omega)$  has both real and imaginary parts when  $|U - n\omega| < 4\bar{t}_h\sqrt{z-1}$ ; the real part contributes to the ordinary exchange parameter, while the imaginary part can be related to the doublon-holon creation rate at bond  $\langle ij \rangle$  and thus also to the increase in the local density of DH pairs. From Fig. 1 it is inferred that the imaginary part of  $g_{\text{dh}}$  is always positive; this along with the fact that the effective Hamiltonian has a term like  $\bar{J}_{ij}(-\frac{1}{4} + \mathbf{S}_i \cdot \mathbf{S}_j)$  for every bond guarantees that the creation rate is always

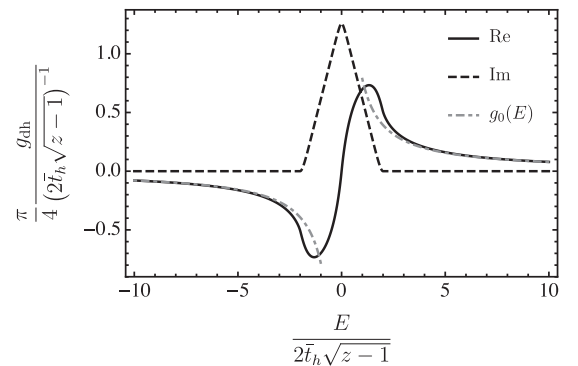


FIG. 1. Real and imaginary parts of the Green's function computed with the retraceable path approximation. The Green's function  $g_0(E) = \frac{1}{E}$  is plotted for reference. The value of  $z = 6$  is chosen for this plot.

positive. In fact the creation rate is zero for neighboring triplets and positive for neighboring singlets. Note that the exchange interaction parameter derived in the previous section [Eq. (13)] by neglecting DH hoppings can be consistently recovered by noting that  $g_{\text{dh}}(U - n\omega)$  behaves similarly to  $\frac{1}{U - n\omega}$  for sufficiently large values of  $(U - n\omega)/(\sqrt{z - 1}\tilde{t}_h)$ .

The above considerations show that the Floquet spin model breaks down when the photon energy  $\omega$  (setting  $\hbar = 1$ ) is in resonance with the interaction energy  $U$ , i.e.,  $n\omega$  is around  $U$ . In such resonant regime, the periodic driving would generate real DH pairs, and the description of the system by the low-energy spin dynamics is no longer valid. As shown in Appendix C and discussed above, the excitation spectrum has a finite bandwidth  $4\sqrt{z - 1}\tilde{t}_h$  due to the hoppings of the DH pairs. As a result of this, within the approximation scheme used here, real DH pairs are generated as long as the frequency is within this excitation band. On the contrary, when  $\omega$  is outside the DH band, the DH creation rate is tiny and the description of the system by an effective Floquet spin Hamiltonian is still valid, but the expression of  $J_{(ij)}$  would be modified due to the DH hoppings.

One can further find an expression for the rate of the local DH pair creation (when close to a resonance) using the above formalism. The imaginary part of  $g_{\text{dh}}$ , when nonzero, has a typical value of order  $\frac{1}{t_h}$ , and this corresponds to an imaginary effective Hamiltonian of order  $t_h$ , and thus a timescale for DH pair creation rate  $\sim \frac{1}{t_h}$ ; while, on the other hand, the timescale for spin dynamics due to the effective Hamiltonian is of order  $\frac{U}{t_h}$ . Clearly, the latter is much larger in the insulating limit. Thus in order to find the DH pair creation rate, we would restrict our attention to the ground-state spin configuration of the static Hamiltonian, which is antiferromagnetic order in our case. In other words, the Floquet spin dynamics which is induced by turning on the laser radiation can safely be neglected. As pointed above, the rate of increase in the density of DH pairs  $\rho_{\text{dh}}$  is basically the doublon creation rate in this spin ground state; this is nothing but the decay rate of the spin ground state calculated using the imaginary part of the Green's function described above and thus takes the following form:

$$\begin{aligned} \frac{\partial}{\partial t} \rho_{\text{dh}} &= \frac{1}{N} \sum_{(ij)} \sum_{n=-\infty}^{\infty} 4t_h^2 \mathcal{J}_n^2(u_{ij}) \text{Im} g_{\text{dh}}(U - n\omega) \\ &\times \langle \Psi_0 | \left[ \frac{1}{4} - \mathbf{S}_i \cdot \mathbf{S}_j \right] | \Psi_0 \rangle. \end{aligned} \quad (21)$$

where one can use the spin ground state of the static Hamiltonian for  $|\Psi_0\rangle$  in this relation. A consistent result can also be derived using Fermi's golden rule.

One should note that in order to take the effect of bandwidth of DH pairs into account we have made a partial summation over virtual hopping processes, while neglecting other terms in the perturbation theory which can be of the same order; this can be justified as follows: Because the hopping parameter is considered small, all these lower-order contributions (including the virtual DH hoppings) play subleading roles when compared to the dominant exchange term which is derived using strict perturbative expansion, unless one is close to a resonance; in this situation the strict

perturbation expansion gives a divergent result, which can be made finite if the higher-order effects of DH virtual hoppings are taken into account, and this corresponds to the terms that are retained in our considerations. Other higher-order corrections, on the other hand, can be argued to have small contributions everywhere. One can also argue in more technical terms that the higher-order contributions that are kept here, i.e., virtual hoppings of the doublon and holon that take the two particles back to their original positions, are present for every process considered. In a diagrammatic perturbation theory language, every virtual hopping process can be dressed by the above contributions at each step, and thus we are in fact calculating the normalized hopping parameter by the partial sum performed here.

### C. Small-frequency regime

With the form (21) for the creation rate of DH pairs at hand, we turn our attention to the study of the doublon creation rate at small frequencies. At very small frequencies, one expects the absorption of a high number of photons for supplying the energy needed for the creation of a DH pair, as a result of this one expects large values of  $n$  (of order  $U/\omega$ ) to only contribute to the sum in Eq. (21). One can further justify this point by noting that the function  $\text{Im} g_{\text{dh}}(U - n\omega)$  in (21) is nonzero when its argument is in a window around 0 (Fig. 1), and thus only terms with  $n \sim U/\omega$  contribute to the sum.

Turning to the Bessel function in the sum, we note that a Bessel function of large order is essentially zero until its argument gets comparable to its order, and this can be seen by checking the integral representation of a Bessel function  $\mathcal{J}_n(A) = \frac{\omega}{2\pi} \int_0^{2\pi/\omega} dt e^{iA \sin \omega t} e^{-in\omega t}$ ; when  $n$  is large and  $A$  is not, the factor  $e^{-in\omega t}$  oscillates rapidly and in one of its periods,  $e^{iA \sin \omega t}$  is almost constant, which makes the integral negligible. The integral becomes not very small only when  $A$  becomes comparable to  $n$ . As argued above,  $n$  should be of order  $U/\omega$  and thus noting that the argument of the Bessel functions in (21) is  $u_{ij} = eEa/\omega$ , with  $a$  being the lattice constant, one needs  $eEa \sim U$  for a non-negligible absorption.

To present a more accurate treatment, we will focus on a given bond and assume that the spins on the two ends of the bond are aligned antiferromagnetically. The change in the local density of DH pairs due to creation of a pair at the two ends of a given bond  $\langle ij \rangle$  reads [46]:

$$\frac{\partial}{\partial t} \rho_{\text{dh}} = \sum_{n=-\infty}^{\infty} 4t_h^2 \mathcal{J}_n^2(u_{ij}) \text{Im} g_{\text{dh}}(U - n\omega) \times \frac{1}{2}. \quad (22)$$

The site indices will be suppressed in the what follows. First, we present a numerical evaluation of the sum in (22) for small values of  $\omega$ , and different values of the electric field energy  $\Phi = eEa = u\omega$ .

The rate of change in the density of DH pairs given by Eq. (22) is evaluated numerically for a range of small frequencies, while the electric field energy is varied. In this section, all energies are expressed in units of  $2t_h\sqrt{z - 1}$  and all times in units of its inverse. A plot of DH creation rate for  $U = 10$  can be found in Fig. 2. Figure 2 shows that among many field-dependent behaviors, something similar happens for different field energies at very small frequencies:

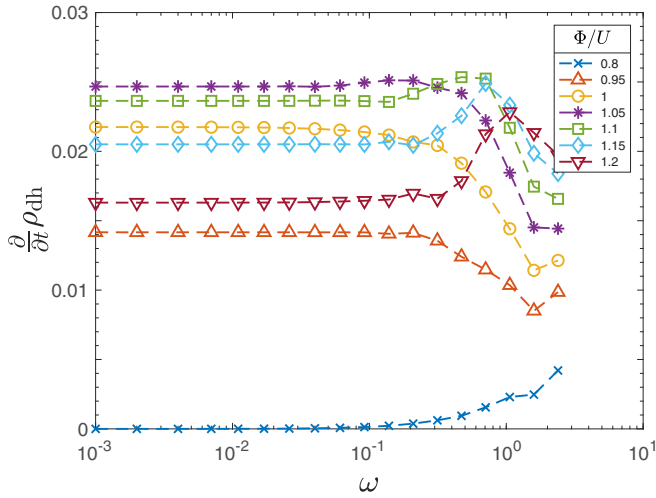


FIG. 2. Semilogarithmic plot of DH pair creation rate at a given bond. This plot shows how the DH creation rate behaves for small frequencies for different values of electric field energy near  $U = 10$ . All energies are expressed in units of  $2t_h\sqrt{z-1}$  and thus  $\frac{1}{2t_h\sqrt{z-1}} \frac{\partial}{\partial t} \rho_{\text{dh}}$  versus  $\frac{\omega}{2t_h\sqrt{z-1}}$  is actually plotted here.

The creation rate shows a saturation for different values of field energy, i.e., a constant value is maintained over two orders of magnitude of change in frequency. This suggests the possibility for existence of a zero-frequency limit in the DH pair creation rate.

The small-frequency saturation value can be extracted numerically for different electric field strengths, a plot of which is presented in Fig. 3 as the data points. First, this plot shows that a nonvanishing zero-frequency limit exists only if  $\Phi/U \geq 0.8$ , i.e., when the electric field energy is above the lower bound of the DH excitations, and below this value it is

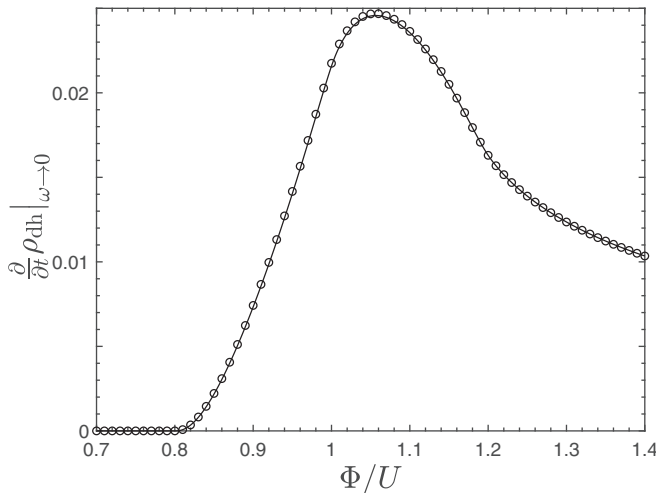


FIG. 3. The zero-frequency limit of DH creation rate plotted as a function of electric field strength. The data points correspond to the values of zero-frequency limit, obtained by finding the saturation values at small frequencies for different field strengths numerically. The solid line, on the other hand, shows the prediction of the analytical result (24). This shows that there is a very good agreement between the two results.

negligible (zero within our approach). Second, it also shows that the maximum zero-frequency limit of the DH creation rate occurs at an electric field strength just slightly higher than  $U$ . This zero-frequency limit of DH creation rate can also be interpreted as the rate for the breakdown of a Mott insulator, when exposed to a static electric field and thus we indeed expect from Fig. 3 that the maximum static breakdown rate happens when  $\Phi$  is very close to  $U$ .

We then turn our focus to an analytical study of the asymptotic behavior of the sum in Eq. (22). Since the imaginary part of the Green's function  $g_{\text{dh}}(E)$  is only nonzero when its argument sits in the window  $(U - 2, U + 2)$ , the sum can be rewritten as:

$$\begin{aligned} \mathcal{S} &= \sum_{n=-\infty}^{\infty} \mathcal{J}_n^2(\Phi/\omega) \text{Im}g_{\text{dh}}(U - n\omega) \\ &= \sum_{n \sim U/\omega - 2/\omega}^{U/\omega + 2/\omega} \mathcal{J}_n^2(\Phi/\omega) \text{Im}g_{\text{dh}}(U - n\omega). \end{aligned} \quad (23)$$

In the limit of very small frequency,  $n$  is a large number for all the terms in the above sum, and thus one can use an asymptotic form for Bessel functions of high order (Appendix D). After substituting the Bessel functions with the asymptotic forms, the sum can further be converted to an integral, and thus finally the quantity  $\mathcal{S}$  in the zero-frequency limit takes the form (Appendix D):

$$\lim_{\omega \rightarrow 0} \mathcal{S} = \frac{1}{\pi} \int_{U-2}^{\Phi} d\bar{v} \left[ \frac{1}{\left(\frac{\Phi}{\bar{v}}\right)^2 - 1} \right]^{1/2} \frac{1}{\bar{v}} \text{Im}g_{\text{dh}}(U - \bar{v}). \quad (24)$$

This analytical form for the zero-frequency limit is plotted and compared to the numerical result in Fig. 3 as the solid line, and it can be seen that there is a very good agreement between this analytical result and the saturation values found numerically. Indeed, this shows that there is a zero-frequency limit for the creation rate of DH pairs and thus, as mentioned above, the breakdown rate of the Mott insulator due to a static electric field can be read from Fig. 3. These results can be easily generalized to the multiorbital Mott insulators by the treatments introduced in Sec. III B.

### III. FLOQUET SPIN-ORBITAL MODEL

#### A. Time-dependent perturbation theory

The previous discussion of the periodically driven Hubbard model can be generalized to the case of periodically driven multiorbital Mott insulators with Kanamori local interactions [47]

$$\begin{aligned} H_K &= U \sum_{i,\alpha} \hat{n}_{i\alpha\uparrow} \hat{n}_{i\alpha\downarrow} + U' \sum_{i,\alpha < \beta, \sigma, \sigma'} \hat{n}_{i\alpha\sigma} \hat{n}_{i\beta\sigma'} \\ &\quad - J_H \sum_{i,\alpha < \beta, \sigma, \sigma'} c_{i\alpha\sigma}^\dagger c_{i\alpha\sigma'} c_{i\beta\sigma'}^\dagger c_{i\beta\sigma} \\ &\quad + J_P \sum_{i,\alpha < \beta, \sigma} c_{i\alpha\sigma}^\dagger c_{i\alpha-\sigma}^\dagger c_{i\beta\sigma} c_{i\beta-\sigma}, \end{aligned} \quad (25)$$

where  $U$  and  $U'$  are the intraorbital and interorbital direct Coulomb interactions.  $J_H$  and  $J_P$  denote the onsite exchange

interaction (Hunds's coupling) and the pair hopping respectively; the sets of indices  $\{i, j\}$ ,  $\{\alpha, \beta\}$ ,  $\{\sigma, \sigma'\}$  denote the lattice sites, orbitals, and spin degrees of freedom. As in the case of the Hubbard model, the effect of the laser radiation is manifested in the kinetic energy via the so-called Peierls substitution,

$$T_t = \sum_{(ij), \alpha\beta, \sigma} (t_{i\alpha, j\beta} e^{iu_{ij} \sin \omega t} c_{i\alpha\sigma}^\dagger c_{j\beta\sigma} + \text{H.c.}), \quad (26)$$

where  $t_{i\alpha, j\beta}$  represents the hopping amplitude from orbital  $\beta$  at site  $j$  to orbital  $\alpha$  at site  $i$ . Note that Hermiticity dictates  $t_{i\alpha, j\beta} = t_{j\beta, i\alpha}^*$ , along with  $u_{ij} = -u_{ji}$ .

In the multiorbital case, we also need to consider the crystal-field splittings ( $H_{\text{CF}}$ ). In addition to the giant  $t_{2g} - e_g$  splitting in typical perovskite transition-metal oxides, there may be additional splittings within the  $t_{2g}$  and/or  $e_g$  manifold due to the octahedral rotations, tiltings [48], and Jahn-Teller distortions [40]. The crystal-field splitting between  $t_{2g}$  and  $e_g$  levels is on the order of a few eV, but the splittings due to octahedral rotations and Jahn-Teller distortions are typically much smaller. Throughout this paper we only consider the  $t_{2g}$  orbitals. Within the quasidegenerate  $t_{2g}$  levels we further include the crystal-field splittings from various octahedral distortions and tiltings,

$$H_{\text{CF}} = \sum_i \sum_{\alpha, \beta, \sigma} \epsilon_{i, \alpha\beta} c_{i\alpha\sigma}^\dagger c_{i\beta\sigma}. \quad (27)$$

Including all these terms, we find the total periodically driven Hamiltonian as  $H_t = T_t + H_K + H_{\text{CF}}$ .

We consider the limit that the typical interaction energy scale (a few eV) is much greater than the hopping energy scale ( $\sim 0.1$  eV in  $3d$  transition-metal oxides) and consider  $T_t$  as a perturbation to  $H_K$ . In the nondriven case, the low-energy physics is dominated by the spin and orbital dynamics, which is well described by the Kugel-Khomskii [40,49] and similar spin-orbital models and can be derived using time-independent second-order perturbation theory. Doubly occupied states have different energies for different spin and orbital configurations. We also neglect the  $H_{\text{CF}}$  in the calculation of energies of the virtual double-occupancy states, since  $H_{\text{CF}}$  has a much smaller energy scale than  $H_K$ .

To find an effective equation of motion in this model, in an approach similar to the one used in the single-orbital case, we expand a generic state of the system in terms of the states with different numbers of double occupancies. We then truncate the equations of motion similarly to arrive at:

$$\begin{aligned} i\partial_t |\Psi_0\rangle_t &= \hat{P}_0 T_t |\Psi_1\rangle_t, \\ i\partial_t |\Psi_1\rangle_t &= H_K |\Psi_1\rangle_t + T_t |\Psi_0\rangle_t + \tilde{T}_t |\Psi_1\rangle_t. \end{aligned} \quad (28)$$

where  $\tilde{T} = \hat{P}_1 T_t \hat{P}_1$ , and the hopping operator  $T_t$  in this case is multiorbital. First, we consider the case where the effect of hopping of virtual excitations is negligible, which occurs when one is sufficiently away from a resonance. In this case, one can safely drop the term  $\hat{P}_1 T_t |\Psi_1\rangle_t$  in the second equation of (28), and with the same manipulations done in the single-orbital case, one arrives at the following form for the effective

equation of motion of  $|\Psi_0\rangle_t$ :

$$\begin{aligned} i\partial_t |\Psi_0\rangle_t &= - \sum_{n,m} \sum_{(ij)} \mathcal{J}_n(u_{ji}) \mathcal{J}_m(u_{ij}) e^{i(m-n)\omega t} \\ &\times \sum_{\alpha\beta\sigma\alpha'\beta'\sigma'} t_{i\alpha j\beta} t_{j\alpha' i\beta'} c_{j\alpha'\sigma'}^\dagger c_{i\beta\sigma} \\ &\times \frac{1}{H_K - n\omega} c_{i\alpha\sigma}^\dagger c_{j\beta\sigma} |\Psi_0\rangle_t + (i \leftrightarrow j), \end{aligned} \quad (29)$$

where  $H_K$  is the Kanamori interaction operator defined in (25).

The Floquet spin-orbital effective Hamiltonian can now be obtained by time averaging:

$$H^{\text{eff}} = \sum_n \sum_{(ij)} \mathcal{J}_n^2(u_{ij}) \hat{\Lambda}_{ij}(n\omega), \quad (30)$$

with  $\hat{\Lambda}_{ij}$  defined as:

$$\begin{aligned} \hat{\Lambda}_{ij}(n\omega) &= - \left[ \sum \left( t_{i\alpha j\beta} t_{j\alpha' i\beta'} c_{j\alpha'\sigma'}^\dagger c_{i\beta\sigma} \frac{1}{H_K - n\omega} c_{i\alpha\sigma}^\dagger c_{j\beta\sigma} \right) \right. \\ &\left. + (i \leftrightarrow j) \right] \hat{P}_0, \end{aligned} \quad (31)$$

with the summation done over the set of indices  $\{\alpha, \beta, \sigma, \alpha', \beta', \sigma'\}$ . To calculate the operator  $\hat{\Lambda}_{ij}$ , one should note that it creates a doublon-holon pair at sites  $i, j$ , then acts on the resulting state with the inverse Kanamori Hamiltonian, and, finally, annihilates the pair. It is a 0-doublon-to-0-doublon operator and thus can be written in terms of spin and orbital operators acting on the 0-doublon subspace. As mentioned above we will compute this operator for the case of three orbitals.

Noting that  $H_K$  has four distinct eigenvalues  $E_{K,1} = U' - J_H$ ,  $E_{K,2} = U' + J_H$ ,  $E_{K,3} = U - J_P$ ,  $E_{K,4} = U + 2J_P$ , one is able to expand  $\hat{\Lambda}_{ij}(n\omega)$  as follows:

$$\begin{aligned} \hat{\Lambda}_{ij}(n\omega) &= \frac{\hat{\Lambda}_{ij,1}}{U' - J_H - n\omega} + \frac{\hat{\Lambda}_{ij,2}}{U' + J_H - n\omega} \\ &+ \frac{\hat{\Lambda}_{ij,3}}{U - J_P - n\omega} + \frac{\hat{\Lambda}_{ij,4}}{U + 2J_P - n\omega}, \end{aligned} \quad (32)$$

where  $\hat{\Lambda}_{ij,m}$  is the spin-orbital operator corresponding to eigenvalue number  $m$ . One can further decompose these operators into spin and orbital parts as follows:

$$\begin{aligned} \hat{\Lambda}_{ij,1} &= \left(\frac{3}{4} + \mathbf{S}_i \cdot \mathbf{S}_j\right) [\hat{\gamma}_{ij,2} - \hat{\gamma}_{ij,1}], \\ \hat{\Lambda}_{ij,2} &= \left(-\frac{1}{4} + \mathbf{S}_i \cdot \mathbf{S}_j\right) [\hat{\gamma}_{ij,2} + \hat{\gamma}_{ij,1} - \hat{\gamma}_{ij,3}], \\ \hat{\Lambda}_{ij,3} &= \left(-\frac{1}{4} + \mathbf{S}_i \cdot \mathbf{S}_j\right) [\hat{\gamma}_{ij,3} - \hat{\gamma}_{ij,4}], \\ \hat{\Lambda}_{ij,4} &= \left(-\frac{1}{4} + \mathbf{S}_i \cdot \mathbf{S}_j\right) \hat{\gamma}_{ij,4}. \end{aligned} \quad (33)$$

In the above equations,  $\gamma_{ij,m}$  are the following orbital operators:

$$\begin{aligned} \hat{\gamma}_{ij,1} &= \sum_{\alpha_i\beta_i\beta_j} \hat{A}_{\alpha_i\beta_i}^i t_{i\alpha_i j\beta_j} t_{j\beta_j i\beta_i} + (i \leftrightarrow j), \\ \hat{\gamma}_{ij,2} &= 2 \sum_{\alpha_i\beta_i\alpha_j\beta_j} \hat{A}_{\alpha_i\beta_i}^i \hat{A}_{\alpha_j\beta_j}^j t_{i\alpha_i j\beta_j} t_{j\alpha_j i\beta_i}, \end{aligned}$$



$$\hat{\gamma}_{ij,3} = 2 \sum_{\alpha_i \beta_i \alpha_j} \hat{A}_{\alpha_i \beta_i}^i \hat{A}_{\alpha_j \beta_j}^j t_{i\alpha_i j \alpha_j} t_{j\alpha_j i \beta_i} + (i \leftrightarrow j),$$

$$\hat{\gamma}_{ij,4} = \frac{2}{3} \sum_{\alpha_i \beta_i \alpha_j \beta_j} \hat{A}_{\alpha_i \beta_i}^i \hat{A}_{\alpha_j \beta_j}^j t_{i\alpha_i j \alpha_j} t_{j\beta_j i \beta_i} + (i \leftrightarrow j). \quad (34)$$

We have introduced the orbital operators  $\hat{A}_{\alpha_i \beta_i}^i = \sum_{\sigma} c_{i\alpha_i \sigma}^{\dagger} c_{i\beta_i \sigma} \hat{P}_0^i$ , with  $\alpha_i, \beta_i = 1, 2, 3$ , as a basis for orbital operations at each site  $i$ , that contains only one electron. Note that  $\hat{P}_0^i$  is the projector onto the states with one electron at site  $i$ . With the above manipulations one is able to derive an effective exchange  $\hat{J}_{ij}$ , which is an orbital operator in the present case:

$$\hat{J}_{ij} = \sum_{n=-\infty}^{\infty} \mathcal{J}_n^2(u_{ij}) \left\{ \frac{\hat{\gamma}_{ij,2} - \hat{\gamma}_{ij,1}}{U' - J_H - n\omega} + \frac{\hat{\gamma}_{ij,2} + \hat{\gamma}_{ij,1} - \hat{\gamma}_{ij,3}}{U' + J_H - n\omega} \right. \\ \left. + \frac{\hat{\gamma}_{ij,3} - \hat{\gamma}_{ij,4}}{U - J_P - n\omega} + \frac{\hat{\gamma}_{ij,4}}{U + 2J_P - n\omega} \right\}. \quad (35)$$

It can be seen from (33) that the last three contributions only arise when the adjacent spins at  $\langle ij \rangle$  are in a singlet state, which means that the virtual processes responsible for these terms only occur when the state of the adjacent spins is a singlet.

It is also worthwhile to study the special case  $U' = U - J_H$  and  $J_P = 0$  [42]. With such an assumption  $H_K$  is rotationally invariant and there are only two distinct multiplet energy levels:  $E_{\text{singlet}} = U$  for spin singlets and  $E_{\text{triplet}} = U - 2J_H$  for spin triplets [42]. Indeed, with this assumption  $E_{K,1} = U - 2J_H$  and  $E_{K,2} = E_{K,3} = E_{K,4} = U$ , and the effective exchange operator becomes

$$\hat{J}_{ij} = \sum_{n=-\infty}^{\infty} \mathcal{J}_n^2(u_{ij}) \left( \frac{\hat{\gamma}_{ij,2} - \hat{\gamma}_{ij,1}}{U - 2J_H - n\omega} + \frac{\hat{\gamma}_{ij,2} + \hat{\gamma}_{ij,1}}{U - n\omega} \right). \quad (36)$$

## B. Bandwidth of excitations

Now we will take into account the effects of the multi-orbital doublon-holon bandwidth. This is quite complex in comparison to the single-orbital Hubbard model and we will, consequently, make a number of simplifying assumptions in order to obtain a tractable result. While these approximations are not fully controlled, we believe they do not qualitatively affect the results. First, we specialize in this part to the case  $U' = U - J_H$  and  $J_P = 0$  and note again that in this case there are only two different eigenvalues for the Kanamori Hamiltonian corresponding to singlet and triplet virtual states:  $E_{\text{singlet}} = U$  and  $E_{\text{triplet}} = U - 2J_H$ .

We have to consider the multi-orbital equations of motion (28) once more and this time we will not neglect the hopping term for the excitations to see the effect of finite bandwidth of excitations in the multi-orbital model. To this end, we expand the 1-doublon component as  $|\Psi_1\rangle_t = |\Psi_1^s\rangle_t + |\Psi_1^t\rangle_t$ , where  $|\Psi_1^s\rangle_t$  and  $|\Psi_1^t\rangle_t$  denote the single-doublon states with their doublon in a spin-singlet state and a spin-triplet state. As discussed before, we neglect the excited states with more than one doublon. The equations of motion can be written as:

$$i\partial_t |\Psi_0\rangle_t = \hat{P}_0 T_i (|\Psi_1^s\rangle_t + |\Psi_1^t\rangle_t),$$

$$i\partial_t |\Psi_1^s\rangle_t = U |\Psi_1^s\rangle_t + \hat{P}_1^s T_i |\Psi_0\rangle_t + \tilde{T}_i^{ss} |\Psi_1^s\rangle_t + \tilde{T}_i^{st} |\Psi_1^t\rangle_t,$$

$$i\partial_t |\Psi_1^t\rangle_t = (U - 2J_H) |\Psi_1^t\rangle_t + \hat{P}_1^t T_i |\Psi_0\rangle_t \\ + \tilde{T}_i^{tt} |\Psi_1^t\rangle_t + \tilde{T}_i^{ts} |\Psi_1^s\rangle_t. \quad (37)$$

Here  $\hat{P}_1^t$  and  $\hat{P}_1^s$  are the triplet and singlet projection operators. The hopping operators are defined as  $\tilde{T}_i^{ab} = \hat{P}_1^a \tilde{T}_i \hat{P}_1^b$  ( $a, b = s, t$ ). We continue by replacing  $\tilde{T}_i^{tt}$  and  $\tilde{T}_i^{ss}$  by their time averages, similarly to the single-orbital case, and also by neglecting the two cross hoppings  $\tilde{T}_i^{st}$  and  $\tilde{T}_i^{ts}$  (see Appendix A). One is now able to write down the 1-doublon components in terms of the 0-doublon component at arbitrary time, and through manipulations similar to those in the single-orbital case one arrives at the following form for the time evolution equation of  $|\Psi_0\rangle_t$  in the multi-orbital case:

$$i\partial_t |\Psi_0\rangle_t = \sum_{\langle ij \rangle (i'j'), mn, a} \{ [f_{i'j'ij}^{mn}(t) \hat{G}_{i'j'ij}^a(n\omega) |\Psi_0\rangle_t] \\ + (i \leftrightarrow j) \} + [i' \leftrightarrow j'] + H_{\text{CF}} |\Psi_0\rangle_t, \quad (38)$$

where  $f_{i'j'ij}^{mn}(t) = -e^{i(m-n)\omega t} \mathcal{J}_m(u_{i'j'}) \mathcal{J}_{-n}(u_{ij})$ , and the index  $a$  in the sum runs over  $\{s, t\}$ . Note that we did not include the  $H_{\text{CF}}$  term in Eq. (37), as we are neglecting it compared to  $H_K$ , but it has been included in (38). The operator  $\hat{G}_{i'j'ij}^a(n\omega)$  is defined as

$$\hat{G}_{i'j'ij}^s(n\omega) = \sum_{\alpha\beta\alpha'\beta', \sigma\sigma'} (t_{i\alpha, j\beta} t_{i'\beta', j'\alpha'}) \hat{P}_0 c_{i'\beta'\sigma'}^{\dagger} c_{j'\alpha'\sigma'} \\ \times (U - n\omega + \bar{T}^{ss})^{-1} \hat{P}_1^s c_{i\alpha\sigma}^{\dagger} c_{j\beta\sigma} \hat{P}_0, \quad (39)$$

$$\hat{G}_{i'j'ij}^t(n\omega) = \sum_{\alpha\beta\alpha'\beta', \sigma\sigma'} (t_{i\alpha, j\beta} t_{i'\beta', j'\alpha'}) \hat{P}_0 c_{i'\beta'\sigma'}^{\dagger} c_{j'\alpha'\sigma'} \\ \times (U - 2J_H - n\omega + \bar{T}^{tt})^{-1} \hat{P}_1^t c_{i\alpha\sigma}^{\dagger} c_{j\beta\sigma} \hat{P}_0.$$

Similarly to the single-orbital case, we also make the following assumption for the operators  $\hat{G}_{i'j'ij}^s$  and  $\hat{G}_{i'j'ij}^t$ : We only consider the hopping processes which create DH pairs at the given sites, propagate them around and bring them to their initial positions and annihilate them, with a final *spin-orbital* configuration which is identical to the initial configuration. Under this assumption, Eq. (39) can be expressed as

$$\hat{G}_{i'j'ij}^a(n\omega) = \sum_{\alpha\beta\alpha'\beta', \sigma\sigma'} t_{i\alpha, j\beta} t_{j'\beta', i'\alpha'} g_{\text{dh}}^a(U^a - n\omega) \\ \times \hat{P}_0 c_{j'\beta'\sigma'}^{\dagger} c_{i'\alpha'\sigma'} \hat{P}_1^a c_{i\alpha\sigma}^{\dagger} c_{j\beta\sigma} \hat{P}_0, \quad (40)$$

with  $a$  being either  $s$  or  $t$ , with  $U^s = U$  and  $U^t = U - 2J_H$  and where

$$g_{\text{dh}}^s(U - n\omega) = \langle \Psi_0 | c_{j\beta\sigma}^{\dagger} c_{i\alpha\sigma} \frac{\hat{P}_1^s}{U - n\omega + \bar{T}^{ss}} c_{i\alpha\sigma}^{\dagger} c_{j\beta\sigma} | \Psi_0 \rangle,$$

$$g_{\text{dh}}^t(U - 2J_H - n\omega) = \langle \Psi_0 | c_{j\beta\sigma}^{\dagger} c_{i\alpha\sigma} \\ \times \frac{\hat{P}_1^t}{U - 2J_H - n\omega + \bar{T}^{tt}} c_{i\alpha\sigma}^{\dagger} c_{j\beta\sigma} | \Psi_0 \rangle. \quad (41)$$

In the multi-orbital case,  $g_{\text{dh}}^{t(s)}$  is calculated using the analogs of Eqs. (17) and (18), assuming the motions of the doublons

and holons are uncorrelated:

$$g_{\text{dh}}^{t(s)}(E - i\delta) = -i \int \frac{d\Omega}{2\pi} g_h(\Omega - i\delta) g_d^{t(s)}(E - \Omega - i\delta), \quad (42)$$

where  $g_h$  and  $g_d^{t(s)}$  are the holon and the doublon Green's functions which are defined in a similar fashion to the single-orbital case:

$$g_h(E - i\delta) = \langle \Psi_0 | c_{j\beta\sigma}^\dagger \frac{1}{E + \bar{T}_h - i\delta} c_{j\beta\sigma} | \Psi_0 \rangle, \\ g_d^{t(s)}(E - i\delta) = \langle \Psi_0 | c_{i\alpha\sigma} \frac{\hat{P}_{1d}^a}{E + \bar{T}_d^{t(s)} - i\delta} c_{i\alpha\sigma}^\dagger | \Psi_0 \rangle, \quad (43)$$

where  $\hat{P}_{1d}^a$  projects onto subspace with zero holon and one  $a$ -type doublon and like the single-orbital case, we have assumed a decomposition for the hopping operator  $\bar{T}^{aa} = \bar{T}_d^a + \bar{T}_h$ . We will try to compute the doublon and the holon Green's functions using the retraceable path approximation in a similar approach to the one presented in Sec. II. One should note that the multiorbital case  $g_h$  and  $g_d$  defined above, unlike the single-orbital model, highly depends on the state in question. In other words, since there are orbital degrees of freedom, even with the RP approximation  $g_h$  and  $g_d^{t(s)}$  do not turn out to be independent of the state  $|\Psi_0\rangle$  since in general hopping parameters can be different for hopping events between different initial and final orbitals.

Noting the above fact, we work in a limit that the crystal-field splitting (within the  $t_{2g}$  or  $e_g$  manifold) is much larger than the intersite exchange energy, so that the occupied orbital at each site is uniquely determined by the crystal-field term and is denoted by the orbital index  $\alpha = 1$ . We would like to consider an effective holon hopping parameter between two adjacent lattice sites  $i$  and  $j$  as an input to our Green's functions calculated using RP approximation; in the classical-orbital regime discussed above, it is legitimate to introduce an effective hopping which accounts for hoppings from orbitals  $|1\rangle_{i(j)}$  to  $|\alpha\rangle_{j(i)}$  and then back, which is denoted as  $t_{ij}^{\text{eff}}$ :

$$(t_{ij}^{\text{eff}})^2 = \frac{1}{2} \sum_{\alpha} (|t_{i1,j\alpha}|^2 + |t_{j1,i\alpha}|^2). \quad (44)$$

In a semiclassical approximation the doublon effective hopping for both of the cases  $(s, t)$  is also taken to be equal to the above value. The effective hopping defined above is anisotropic along different bond directions in general and, furthermore, time averaging  $[\bar{T}^{ss(tt)}]$  introduces a factor of  $\mathcal{J}_0(u_{ij})$  into the hopping amplitudes. For simplicity we further average over the hopping amplitudes along different bond directions, resulting in an effective isotropic DH hopping parameter for a given site  $i$ :

$$\bar{t}_i = \frac{1}{z} \sum_{j \in \text{n.n.}} t_{ij}^{\text{eff}} \mathcal{J}_0(u_{ij}), \quad (45)$$

where "n.n." is the abbreviation for nearest neighbor. One calculates the Green's functions on the right-hand side of (42) with this value of hopping: With this prescription the DH Green's functions for both singlet and triplet cases, i.e.,  $g_{\text{dh}}^s$  and  $g_{\text{dh}}^t$ , will have the same form, and this form agrees with the one discussed in the single-orbital case, except for a different

effective hopping here; the imaginary and real parts of such Green's functions can be found in Fig. 1.

With all this at hand, using manipulations similar to those leading to (35) and (36), one is able to write down the effective Hamiltonian describing the dynamics of the 0-doublon subspace for the multiorbital case which includes the effect of bandwidth of excitations:

$$H^{\text{eff}} = \sum_{(ij),n} \left[ \mathcal{J}_n^2(u_{ij}) (\hat{\gamma}_{ij,2} + \hat{\gamma}_{ij,1}) g_{\text{dh}}^s(U - n\omega) \right. \\ \times \left( -\frac{1}{4} + \mathbf{S}_i \cdot \mathbf{S}_j \right) \\ + \mathcal{J}_n^2(u_{ij}) (\hat{\gamma}_{ij,2} - \hat{\gamma}_{ij,1}) g_{\text{dh}}^t(U - 2J_H - n\omega) \\ \left. \times \left( \frac{3}{4} + \mathbf{S}_i \cdot \mathbf{S}_j \right) \right], \quad (46)$$

in which we have used the orbital operators defined in (34).

It is worthwhile here to make a connection with our result for the multiorbital case when the frequency is away from resonances, i.e., Eq. (36). The functional form for the Green's functions used in the above effective Hamiltonian can be seen in Fig. 1. As we discussed for the single-orbital case, when the argument of the Green's function is much larger than the effective hopping, and hence one is away from a resonance, the Green's functions  $g_{\text{dh}}^a(U^a - n\omega)$  look very similar to  $1/(U^a - n\omega)$ , and thus one recovers the previous form (36). Furthermore, when this argument is close enough to zero, or, more precisely, in a window of width of the same order as the effective hopping, one expects to see a nonzero imaginary part for the Green's function; this can happen when one of the excitation energies is close enough to a multiple of the frequency. Because the Green's function is complex, the above effective Hamiltonian becomes non-Hermitian and thus the effective evolution of  $|\Psi_0\rangle_t$  becomes nonunitary. The stronger this nonunitarity becomes, the more doublons are created. Indeed, a DH pair creation rate for the multiorbital case can also be derived given a spin-orbital configuration which will look similar to the one derived for the single-orbital case (21).

In order for the Floquet engineering of the spin-orbital dynamics to be relevant, one needs to be in a regime where not many doublons are created and thus one needs to avoid certain ranges of parameters in which the nonunitarity of the effective Hamiltonian results in a large rate of doublon creation. Let us consider a concrete example to show how one can study this quantitatively: As mentioned, the above effective Hamiltonian is applied to the orthorhombic titanates  $\text{YTiO}_3$  and  $\text{LaTiO}_3$  using first-principles calculations in Ref. [43]. There we show that the effective exchange interaction for neighboring sites can be engineered to a high degree but the effective exchange parameter turns out to be a complex number. This complex exchange parameter can be interpreted as follows: Its real part shows the strength of the physical exchange interaction between neighboring sites and its imaginary part quantifies the rate of change in DH pairs density. Therefore and as we discuss in length in [43], one will be interested in regimes where the real part of the effective exchange parameter is much larger than its imaginary part; this results in a much smaller timescale for the physical exchange interaction

dynamics than the timescale for DH creation. This leads the exchange interaction to be the dominant physical effect in such a setting.

We believe that the above formalism with slight modifications can be applied to many other realistic situations involving driven multiorbital Mott insulators. In this formalism, not only the effect of Floquet engineering can be computed, but also the rate for a channel of heating, i.e., DH pair creation, can be quantitatively evaluated.

One should finally note that all the discussion assumes that the system is prevented from heating due to absorption of photons, i.e., it is kept in the subspace of interest (the lower Hubbard band is considered here). We have only studied one channel of photon absorption and heating in this work, i.e., the one happening due to creation of real DH pairs in the system. However, there can be other absorption mechanisms present that will lead to unwanted heating such as phonon creation, excitation to higher bands, etc. We have not considered the latter mechanisms in this work since these effects depend on the details of the material in question and thus should be considered case by case. On the other hand, the heating due to creation of DH pairs can be studied in a unified fashion for all materials described by a Hubbard model at low energies as considered here. In applications to specific materials, the effect of other unwanted heating channels must also certainly be accounted for.

#### IV. CONCLUSION

In this work, we have studied the effects of coherent laser driving of single-orbital and multiorbital Mott insulators. We have developed the formalism and methods for calculating the Floquet spin and spin-orbital Hamiltonians in single-orbital and multiorbital Mott insulators, respectively. We have shown that the effective exchange interactions are dependent not only on the intrinsic properties of the materials but also on the properties of the laser radiation. The increased number of parameters describing multiorbital physics enriches the possibilities for Floquet engineering in such systems. Applications to the orthorhombic titanates are studied in Ref. [43], where it is shown by realistic calculations that Floquet engineering in these compounds can be implemented to a high extent. In particular, even the sign of the static exchange interaction can be flipped in the Floquet regime if one uses radiation with properly chosen frequency and electric field strength.

We have further argued that if the frequency of the radiation (and its multiples) is kept away from the Hubbard interaction scale, collectively shown as  $U$ , the heating due to creation of doublon-holon pairs can be avoided and an effective spin or spin-orbital (in the multiorbital case) Hamiltonian can capture the physics of the system. In fact, the finite bandwidth of the excitations, i.e., doublon-holon pairs, which we have shown is of order  $\sqrt{z - \Gamma}t_h$ , specifies a window for  $\omega$  around  $U$  which should be avoided so that heating is suppressed. Using this notion, we have given a criterion for how distant one needs the laser frequency to be from the interaction energies in the Hamiltonian describing the material: A complex-valued effective exchange parameter is calculated, with its real part interpreted as the physical exchange interaction strength. One

requires the real part to dominate over the imaginary part in order for the doublon creation to be negligible.

We have also derived relations for the doublon-holon creation rates using the imaginary part of the complex-valued exchange parameter mentioned above. Using these relations, we have additionally studied the rate of creation of doublon-holon pairs in the very small frequency regime and derived a zero-frequency limit of absorption which can be related to the breakdown of the Mott insulator in the presence of a static electric field. The maximum rate occurs when the electric field energy between neighboring sites is comparable to the Hubbard interaction energy scale. This may be observable experimentally. A potentially interesting subject for future theoretical study is the effects of *selective* doublon-holon generation with specific quantum numbers, i.e., preferential generation of singlets or triplets, forming a gas of excitations with controllable internal degrees of freedom. Our equations for the generation rates of these excitations provide a starting point for such a study.

#### ACKNOWLEDGMENTS

K.H. thanks D. Else and M. Kolodrubetz for fruitful discussions. This research was supported by the NSF materials theory program through Grant No. DMR-1818533 (L.B. and K.H.) and the Army Research Office MURI Grant No. ARO W911NF-16-1-0361, Floquet engineering and metastable states (J.L.).

#### APPENDIX A: TIME AVERAGING THE VIRTUAL HOPPINGS

In this Appendix, we justify the time averaging of virtual hoppings in the time-dependent Schrödinger Eqs. (3) and (37) of the main text.

We first consider the single-orbital case. Consider the left-hand side of the second line of Eq. (3) written in a different way:

$$i(\partial_t + iU + i\tilde{T}_t)|\Psi_1\rangle_t = T_t|\Psi_0\rangle_t. \quad (\text{A1})$$

The unitary evolution operator  $S_t = \hat{P}_1 S_t \hat{P}_1$ , defined as satisfying an equation analogous to the above:

$$i(\partial_t + iU + i\tilde{T}_t)S_t = 0, \quad (\text{A2})$$

can be useful, in the sense that if one finds  $S_t$ , the solution to Eq. (A2), with initial condition  $S_{t=0} = 1$  one can write (A1) as:

$$S_t i \partial_t (S_t^{-1} |\Psi_1\rangle_t) = T_t |\Psi_0\rangle_t, \quad (\text{A3})$$

where  $S^{-1}$  only acts on states in the subspace invariant under  $\hat{P}_1$ . The equation of motion of  $S_t$  can be written as:

$$i \partial_t (e^{iUt} S_t) = e^{iUt} \tilde{T}_t e^{-iUt} (e^{iUt} S_t). \quad (\text{A4})$$

This is similar to an interaction picture time evolution. Noting that the exponentials commute with  $\tilde{T}_t$ , one notices that the above equation is of Floquet type and thus the corresponding effective Hamiltonian to leading order is obtained by time averaging [3,4]. This fact can also be seen by the following manipulations. Using the Fourier series for the hopping

operator  $\tilde{T}_t = \sum_n e^{in\omega t} \tilde{T}_n$ , Eq. (A4) reads:

$$i\partial_t(e^{iU t} S_t) = \sum_n e^{in\omega t} \tilde{T}_n(e^{iU t} S_t). \quad (\text{A5})$$

Noting  $\tilde{T}_0 = \bar{T}$ , one has:

$$i e^{-i\bar{T}t} \partial_t[e^{i(U+\bar{T})t} S_t] = \sum_{n \neq 0} e^{in\omega t} \tilde{T}_n(e^{iU t} S_t). \quad (\text{A6})$$

Moving the factor  $e^{-i\bar{T}t}$  to the right-hand side, one can integrate the above equation and do integration by parts on the right-hand side, keeping in mind that the derivative of  $(e^{iU t} S_t)$  is of order  $t_h$  (this is similar to what was done in the main text):

$$\begin{aligned} & i\{[e^{i(U+\bar{T})t'} S_{t'}]_{t'=t} - S_{t'=0}\} \\ &= \sum_{n \neq 0} \frac{1}{i(\bar{T} + n\omega)} \left\{ [e^{i(\bar{T}+n\omega)t'} \tilde{T}_n(e^{iU t'} S_{t'})]_{t'=t} - \tilde{T}_n S_{t'=0} \right. \\ & \quad \left. - \int_0^t dt' e^{i(\bar{T}+n\omega)t'} \tilde{T}_n \partial_{t'}(e^{iU t'} S_{t'}) \right\} \\ &= \mathcal{O}\left(\frac{t_h}{\omega}\right). \end{aligned} \quad (\text{A7})$$

The first line on the right-hand side is of first order and the second line of second order and thus the right-hand side is first order overall.

Finally, the solution can be obtained to leading order:

$$S_t = e^{-i(U+\bar{T})t} + \mathcal{O}\left(\frac{t_h}{\omega}\right), \quad (\text{A8})$$

and plugging this back into (A3), one obtains the desired result.

One can generalize this to the multiorbital case also, noting the fact that the multiorbital doublon can be in a singlet or triplet state and so the following decompositions should be considered:

$$\hat{P}_1 = \hat{P}_1^s + \hat{P}_1^t, \quad \hat{U} = U\hat{P}_1^s + (U - 2J)\hat{P}_1^t, \quad (\text{A9})$$

$$\tilde{T}_t = \tilde{T}_t^{ss} + \tilde{T}_t^{st} + \tilde{T}_t^{ts} + \tilde{T}_t^{tt}, \quad (\text{A10})$$

with  $\tilde{T}_t^{ab} = \hat{P}_1^a \tilde{T}_t \hat{P}_1^b$ . The analog of Eq. (A4), can be written as:

$$\begin{aligned} i\partial_t(e^{i\hat{U}t} \hat{S}_t) &= e^{i\hat{U}t} \tilde{T}_t e^{-i\hat{U}t} (e^{i\hat{U}t} \hat{S}_t) \\ &= [\tilde{T}_t^{ss} + \tilde{T}_t^{tt} + \tilde{T}_t^{ts} e^{i2Jt} + \tilde{T}_t^{st} e^{-i2Jt}] (e^{i\hat{U}t} \hat{S}_t). \end{aligned} \quad (\text{A11})$$

A similar argument like the one carried out for the case of a single orbital can be applied here also, except that when  $2J$  and  $n\omega$  are not close to each other (compared with  $t_h$ ),  $\tilde{T}_t^{ts} e^{i2Jt}$  and  $\tilde{T}_t^{st} e^{-i2Jt}$  do not have constant terms. Thus the final form for  $\hat{S}_t$  reads:

$$\hat{S}_t = e^{-i(\hat{U} + \bar{T}^{ss} + \bar{T}^{tt})t} + \mathcal{O}\left(\frac{t_h}{\omega_0}\right), \quad (\text{A12})$$

where  $t_h$  in  $\mathcal{O}$  show the typical hopping parameter and  $\omega_0$  in the denominator stands for either of  $\omega$  or  $J$ .

## APPENDIX B: OVERVIEW OF THE RETRACEABLE PATH APPROXIMATION

In this Appendix we present a short discussion of the RP approximation of Brinkman and Rice [38]. With the notation of the main text, one can write the Green's function of a single hole in a single band Hubbard model as:

$$\begin{aligned} g_h(E) &= \sum_{\sigma} \langle \Psi_0 | c_{j\sigma}^{\dagger} \frac{1}{E + \bar{T}_h} c_{j\sigma} | \Psi_0 \rangle \\ &= \frac{1}{E} \langle 0 | c_{j\sigma_j}^{\dagger} \left[ 1 + \left(-\frac{\bar{T}_h}{E}\right) + \left(-\frac{\bar{T}_h}{E}\right)^2 \right. \\ & \quad \left. + \left(-\frac{\bar{T}_h}{E}\right)^3 + \dots \right] c_{j\sigma_j} | 0 \rangle. \end{aligned} \quad (\text{B1})$$

Note that  $|\Psi_0\rangle$  has one electron per site and thus the state  $c_{j\sigma_j}|\Psi_0\rangle$  has a hole at site  $j$ , with  $\sigma_j$  showing the spin at site  $j$  in state  $|\Psi_0\rangle$ . The series on the right-hand side shows that one should consider all the possible paths including arbitrary number of holon hoppings that connect the state with a hole to itself. Moreover, the final spin configuration should be the same as the initial. The RP approximation amounts to considering only paths that start at  $j$  and terminate at the same point, with the constraint that the hopping holon should exactly retrace its forward-going path in its way back to the original location. With this constraint, every spin reordering that is done in the forward-going path is corrected when the particle is getting back. What one is missing here is the contribution by the paths that are closed loops and to correct all the spin reorderings in some way.

We use the following ansatz for the one-holon Green function, with the introduction of a self-energy:

$$g_h(E) = \frac{1}{E[1 - \Sigma(E)]}. \quad (\text{B2})$$

Since we are considering paths with any number of hoppings, at each step of a path for the remainder of the path, one should consider all the paths that start at the given point and come back to the same position, except for the one going backward. This is very similar to what we are trying to compute, and thus in order to perform an infinite summation over the retraceable paths, one introduces a summation of all forward-going paths at a specific step of the path. At a given step of the process, since the paths can just go forward, there are  $(z - 1)$  choices for direction of the next step, with  $z$  the coordination number. The following equation for  $\Sigma^A$  will result in a self-consistent summation over forward-going paths with arbitrary lengths, something that is present as the future of every step (other than the first) in a retraceable path:

$$\Sigma^A(E) = \frac{(z-1)t_h^2}{E^2[1 - \Sigma^A(E)]}, \quad (\text{B3})$$

which has the solution:

$$\Sigma^A(E) = \frac{1}{2} \left[ 1 \pm \sqrt{1 - 4(z-1)\frac{t_h^2}{E^2}} \right], \quad (\text{B4})$$

where the hopping parameter in  $\bar{T}_h$  is shown as  $t_h$ . The self-energy can be written in terms of the sum of all the



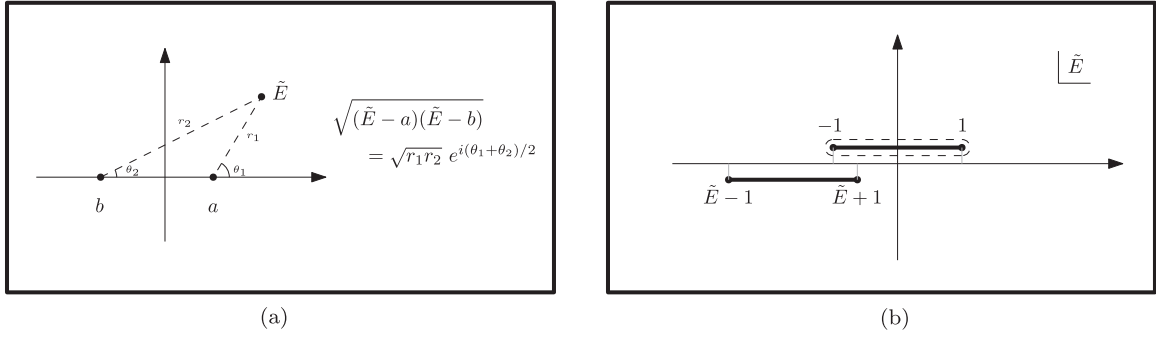


FIG. 4. Appendix C figures. (a) Definition of square root in the complex  $E$  plane; (b) The contour for computing  $g_{\text{dh}}$ .

forward-going paths as:

$$\Sigma(E) = \frac{z}{z-1} \Sigma^A(E), \quad (\text{B5})$$

because at the first step of each path there are  $z$  choices of direction rather than  $z-1$  choices for the holon. This finally results in the following form for the Green's function:

$$g_h(E) = \frac{2(z-1)}{E[(z-2) + z\sqrt{1-4(z-1)t_h^2/E^2}]}. \quad (\text{B6})$$

The solution with a minus sign in Eq. (B4) is chosen so that the above Green's function behaves as  $\frac{1}{E}$  as  $E \rightarrow \infty$ .

One can also consider the case of anisotropic hoppings which results in solving more self-consistent equations. We will work with hopping parameters  $t_\mu$  that are different for different directions. One can further introduce a summation over all the forward-going paths in different directions, denoted as  $\Sigma_\mu^A(E)$ , which should satisfy the following self-consistent equations:

$$\Sigma_\mu^A(E) = \frac{t_\mu^2/E^2}{1 - \Sigma_\mu^A(E) - \sum_{\mu' \neq \mu} \Sigma_{\mu'}^A(E)}, \quad \mu = 1, \dots, d. \quad (\text{B7})$$

The total self-energy used for obtaining the Green's function can be written in terms of the  $\Sigma_\mu^A$  as follows:

$$\Sigma(E) = 2 \sum_{\mu} \Sigma_\mu^A(E). \quad (\text{B8})$$

Case (i)  $\tilde{E} > 2$

$$\left(\frac{\pi}{2} \tilde{t}_h \sqrt{z-1}\right) g_{\text{dh}}(\tilde{E}) = (z-1)^2 z \int_{-1}^1 d\tilde{\Omega} \frac{(1-\tilde{\Omega}^2)^{1/2}}{\tilde{\Omega}^2(-4z+4)+z^2} \frac{1}{(\tilde{E}-\tilde{\Omega})(z-2)+z[(-\tilde{E}+\tilde{\Omega})^2-1]^{1/2}}. \quad (\text{C2})$$

Case (ii)  $\tilde{E} < -2$

$$\left(\frac{\pi}{2} \tilde{t}_h \sqrt{z-1}\right) g_{\text{dh}}(\tilde{E}) = (z-1)^2 z \int_{-1}^1 d\tilde{\Omega} \frac{(1-\tilde{\Omega}^2)^{1/2}}{\tilde{\Omega}^2(-4z+4)+z^2} \frac{1}{(\tilde{E}-\tilde{\Omega})(z-2)-z[(-\tilde{E}+\tilde{\Omega})^2-1]^{1/2}}. \quad (\text{C3})$$

Case (iii)  $0 < \tilde{E} < 2$

$$\begin{aligned} \left(\frac{\pi}{2} \tilde{t}_h \sqrt{z-1}\right) g_{\text{dh}}(\tilde{E}) &= (z-1)^2 z \int_{-1}^{\tilde{E}-1} d\tilde{\Omega} \frac{(1-\tilde{\Omega}^2)^{1/2}}{\tilde{\Omega}^2(-4z+4)+z^2} \frac{1}{(\tilde{E}-\tilde{\Omega})(z-2)+z[(-\tilde{E}+\tilde{\Omega})^2-1]^{1/2}} \\ &+ (z-1)^2 z \int_{\tilde{E}-1}^1 d\tilde{\Omega} \frac{(1-\tilde{\Omega}^2)^{1/2}}{\tilde{\Omega}^2(-4z+4)+z^2} \frac{1}{(\tilde{E}-\tilde{\Omega})(z-2)-iz[1-(-\tilde{E}+\tilde{\Omega})^2]^{1/2}}. \end{aligned} \quad (\text{C4})$$

A first approximation for finding the solution to the above self-consistent equations (B7) would be to use the average hopping  $\sum_{\mu} t_{\mu}$  for every  $t_{\mu}$ ; one can make this approximation better by iterating the solution obtained this way in Eq. (B7).

### APPENDIX C: THE FREQUENCY INTEGRAL OF THE DH GREEN'S FUNCTION

In this Appendix, we show how the convolution integral in Eq. (17) can be calculated in order to get the functional form shown in Fig. 1.

The holon and doublon Green's functions in the RP approximation can be written in the following form as well:

$$g_h(E) = g_d(E) = \frac{2(z-1)}{E(z-2) + z\sqrt{E^2 - 4(z-1)t_h^2}}, \quad (\text{C1})$$

with the definition of the square-root function in the denominator, in the complex  $E$  plane, presented in Fig. 4(a). It is easy to check that with this definition and the signs above, the two Green's functions fall off like  $\frac{1}{E}$  for large  $E$ . Note that we define the dimensionless frequencies as  $\tilde{E} = \frac{E}{2t_h\sqrt{z-1}}$ .

In order to find  $g_{\text{dh}}$ , one should do the frequency integral in Eq. (17), with the integrand having two branch cuts as shown in Fig. 4(b). Using Cauchy's theorem the contour  $(-\infty, \infty)$  can be deformed into a contour that turns around the upper branch cut, and the integral can be done for this contour. In four different ranges for  $E$  the integral over this contour is computed in the following:

Case (iv)  $-2 < \tilde{E} < 0$

$$\begin{aligned} \left(\frac{\pi}{2} \tilde{t}_h \sqrt{z-1}\right) g_{\text{dh}}(\tilde{E}) = & (z-1)^2 z \int_{\tilde{E}+1}^1 d\tilde{\Omega} \frac{(1-\tilde{\Omega}^2)^{1/2}}{\tilde{\Omega}^2(-4z+4)+z^2} \frac{1}{(\tilde{E}-\tilde{\Omega})(z-2)-z[(-\tilde{E}+\tilde{\Omega})^2-1]^{1/2}} \\ & + (z-1)^2 z \int_{-1}^{\tilde{E}+1} d\tilde{\Omega} \frac{(1-\tilde{\Omega}^2)^{1/2}}{\tilde{\Omega}^2(-4z+4)+z^2} \frac{1}{(\tilde{E}-\tilde{\Omega})(z-2)-iz[1-(-\tilde{E}+\tilde{\Omega})^2]^{1/2}}. \end{aligned} \quad (\text{C5})$$

$g_{\text{dh}}$  only has nonzero imaginary part in cases (iii) and (iv). A plot of  $g_{\text{dh}}$ , obtained above, can be found in Fig. 1;  $z = 6$  is taken for this plot.

#### APPENDIX D: ZERO-FREQUENCY LIMIT OF DH PAIRS CREATION RATE

In this Appendix, we present a derivation of the zero-frequency limit of the DH pair creation rate and derive the result (24). We will take the frequency  $\omega$  to be very small. Our starting point is the sum:

$$S = \sum_{n=-\infty}^{\infty} \mathcal{J}_n^2(\Phi/\omega) \text{Im}g_{\text{dh}}(U-n\omega) = \sum_{n \sim U/\omega-2/\omega}^{U/\omega+2/\omega} \mathcal{J}_n^2(\Phi/\omega) \text{Im}g_{\text{dh}}(U-n\omega). \quad (\text{D1})$$

Since  $n$  is a very large number in all of the terms in the above sum, one is able to use the following high-order Bessel function asymptotic form [50,51]:

$$\mathcal{J}_\nu(x) \sim \left[ \frac{4\zeta\left(\frac{x}{\nu}\right)}{1-\left(\frac{x}{\nu}\right)^2} \right]^{1/4} \frac{\text{Ai}\left[\nu^{2/3}\zeta\left(\frac{x}{\nu}\right)\right]}{\nu^{1/3}}, \quad (\text{D2})$$

which holds for large and positive  $\nu$  and positive  $x$  and Ai is the Airy function. The function  $\zeta(z)$  is defined as:

$$\zeta(z) = \begin{cases} \left\{ \frac{3}{2} \left[ \log\left(\frac{\sqrt{1-z^2}+1}{z}\right) - \sqrt{1-z^2} \right] \right\}^{2/3} & z \leq 1, \\ -\left[ \frac{3}{2} \left\{ \sqrt{z^2-1} - \cos^{-1}\left(\frac{1}{z}\right) \right\} \right]^{2/3} & z > 1, \end{cases} \quad (\text{D3})$$

where  $\zeta(z)$  is positive if  $z < 1$  and negative if  $z > 1$ . The function  $\zeta(z)$  is depicted in Fig. 5(a), but we will not need its exact form finally. Plugging the asymptotic form back into Eq. (23) and converting the sum over  $n$  into an integral:

$$\begin{aligned} S &= \int_{U/\omega-2/\omega}^{U/\omega+2/\omega} d\nu \left[ \frac{4\zeta\left(\frac{\Phi}{\omega\nu}\right)}{1-\left(\frac{\Phi}{\omega\nu}\right)^2} \right]^{1/2} \frac{\text{Ai}^2\left[\nu^{2/3}\zeta\left(\frac{\Phi}{\omega\nu}\right)\right]}{\nu^{2/3}} \text{Im}g_{\text{dh}}(U-\nu\omega) \\ &= \int_{U-2}^{U+2} d\bar{\nu} \left[ \frac{4\zeta\left(\frac{\Phi}{\bar{\nu}}\right)}{1-\left(\frac{\Phi}{\bar{\nu}}\right)^2} \right]^{1/2} \frac{1}{\bar{\nu}^{2/3}} \text{Im}g_{\text{dh}}(U-\bar{\nu}) \left\{ \frac{1}{\omega^{1/3}} \text{Ai}^2\left[\bar{\nu}^{2/3}\omega^{-2/3}\zeta\left(\frac{\Phi}{\bar{\nu}}\right)\right] \right\}, \end{aligned} \quad (\text{D4})$$

where the substitution  $\bar{\nu} = \omega\nu$  is done in the second line. Only the expression in the [.] is  $\omega$  dependent, and thus it is the term that should be studied in the limit  $\omega \rightarrow 0$ . The following asymptotic forms for the Airy function with a large argument  $|x| \gg 1$

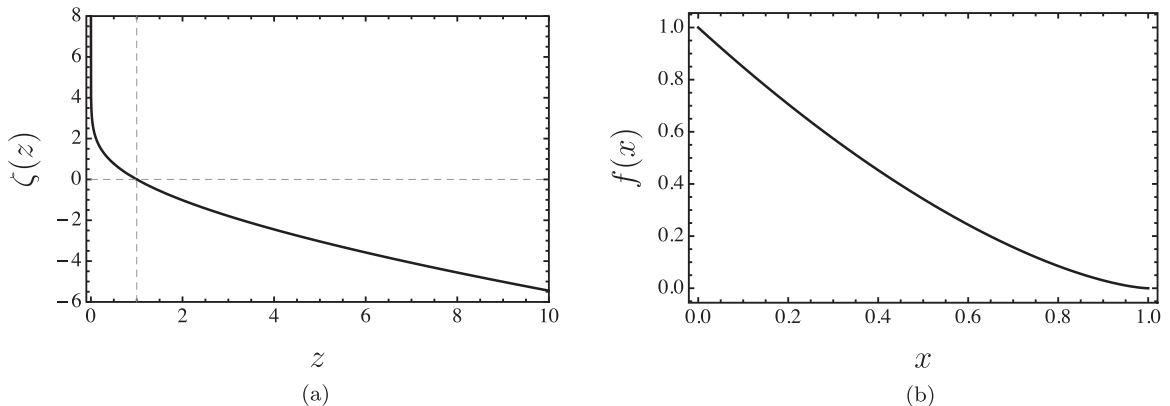


FIG. 5. The two auxiliary functions used in this Appendix. (a) The function  $\zeta(z)$  defined in (D3). It is positive when  $z < 1$  and negative when  $z > 1$  and vanishes at  $z = 0$ ; (b) The function  $f(x) = \sqrt{1-x^2} - x \cos^{-1}(x)$  is a monotonic function for  $0 < x < 1$ .

will be used:

$$\text{Ai}(x) \sim \begin{cases} \frac{1}{2\sqrt{\pi}} x^{-1/4} e^{-\frac{2}{3}x^{3/2}}, & x > 0, \\ \frac{1}{\sqrt{\pi}} (-x)^{-1/4} \sin\left[\frac{2}{3}(-x)^{3/2} + \frac{\pi}{4}\right], & x < 0. \end{cases} \quad (\text{D5})$$

The expression containing  $\omega$  in Eq. (D4) can now be studied in the limit  $\omega \rightarrow 0$  with the above asymptotic forms; for positive values of  $\zeta(\Phi/\bar{v})$  the Airy function decays exponentially in  $1/\omega$ , and thus one should exclude the regions corresponding to  $\zeta(\Phi/\bar{v}) > 0$  in the integral (D4), while for negative values of  $\zeta(\Phi/\bar{v})$  one has:

$$\frac{1}{\omega^{1/3}} \text{Ai}^2\left[\bar{v}^{2/3} \omega^{-2/3} \zeta\left(\frac{\Phi}{\bar{v}}\right)\right] \sim \frac{1}{\omega^{1/3}} \left\{ \frac{\omega^{1/3}}{\pi \bar{v}^{1/3}} \frac{1}{[-\zeta(\Phi/\bar{v})]^{1/2}} \right\} \sin^2\left\{ \frac{2}{3}[-\bar{v}^{2/3} \omega^{-2/3} \zeta(\Phi/\bar{v})]^{3/2} + \frac{\pi}{4} \right\}. \quad (\text{D6})$$

The function  $\zeta$  is negative when its argument is larger than 1, which means  $\Phi > \bar{v}$ . Furthermore, the argument of the  $\sin^2$  function in the above asymptotic form can be rewritten using the definition of  $\zeta$  as:

$$\begin{aligned} \frac{2}{3}[-\bar{v}^{2/3} \omega^{-2/3} \zeta(\Phi/\bar{v})]^{3/2} &= \frac{\bar{v}}{\omega} \frac{2}{3}[-\zeta(\Phi/\bar{v})]^{3/2} \\ &= \frac{\bar{v}}{\omega} \frac{2}{3} \left[ \left( \frac{3}{2} \left\{ \sqrt{(\Phi/\bar{v})^2 - 1} - \cos^{-1}\left[\frac{1}{(\Phi/\bar{v})}\right] \right\} \right)^{2/3} \right]^{3/2} \\ &= \frac{\Phi}{\omega} \left[ \sqrt{1 - \left(\frac{\bar{v}}{\Phi}\right)^2} - \left(\frac{\bar{v}}{\Phi}\right) \cos^{-1}\left(\frac{\bar{v}}{\Phi}\right) \right] \\ &= \frac{\Phi}{\omega} f\left(\frac{\bar{v}}{\Phi}\right). \end{aligned} \quad (\text{D7})$$

The function  $f$  is defined as  $f(x) = \sqrt{1-x^2} - x \cos^{-1}(x)$ . It is a monotonic function of its argument [Fig. 5(b)], when  $0 < x < 1$ , because  $df/dx = -\cos^{-1}(x)$ . We will use this point in what follows. Plugging the asymptotic form back into Eq. (D4), one has:

$$\begin{aligned} \mathcal{S} &= \int_{U-2}^{\Phi} d\bar{v} \left[ \frac{4\zeta(\frac{\Phi}{\bar{v}})}{1 - (\frac{\Phi}{\bar{v}})^2} \right]^{1/2} \frac{1}{\bar{v}^{2/3}} \text{Im}g_{\text{dh}}(U - \bar{v}) \left\{ \frac{1}{\pi \bar{v}^{1/3} [-\zeta(\Phi/\bar{v})]^{1/2}} \right\} \sin^2\left[ \frac{\Phi}{\omega} f\left(\frac{\bar{v}}{\Phi}\right) + \frac{\pi}{4} \right] \\ &= \frac{2}{\pi} \int_{U-2}^{\Phi} d\bar{v} \left[ \frac{1}{(\frac{\Phi}{\bar{v}})^2 - 1} \right]^{1/2} \frac{1}{\bar{v}} \text{Im}g_{\text{dh}}(U - \bar{v}) \sin^2\left[ \frac{\Phi}{\omega} f\left(\frac{\bar{v}}{\Phi}\right) + \frac{\pi}{4} \right]. \end{aligned} \quad (\text{D8})$$

Since the function  $f$  does not have vanishing derivative in the domain of integration, and we are interested in the  $\omega \rightarrow 0$  limit, one can argue that the function  $\sin^2$  oscillates very rapidly and thus can be substituted by its average value  $\frac{1}{2}$ . One finally can write  $\mathcal{S}$  as:

$$\mathcal{S} = \frac{1}{\pi} \int_{U-2}^{\Phi} d\bar{v} \left[ \frac{1}{(\frac{\Phi}{\bar{v}})^2 - 1} \right]^{1/2} \frac{1}{\bar{v}} \text{Im}g_{\text{dh}}(U - \bar{v}). \quad (\text{D9})$$

- [1] J. H. Shirley, *Phys. Rev.* **138**, B979 (1965).
- [2] H. Sambe, *Phys. Rev. A* **7**, 2203 (1973).
- [3] A. Eckardt and E. Anisimovas, *New J. Phys.* **17**, 093039 (2015).
- [4] M. Bukov, L. D'Alessio, and A. Polkovnikov, *Adv. Phys.* **64**, 139 (2015).
- [5] D. Basov, R. Averitt, and D. Hsieh, *Nat. Mater.* **16**, 1077 (2017).
- [6] T. Oka and H. Aoki, *Phys. Rev. B* **79**, 081406(R) (2009).
- [7] T. Kitagawa, T. Oka, A. Brataas, L. Fu, and E. Demler, *Phys. Rev. B* **84**, 235108 (2011).
- [8] N. H. Lindner, G. Refael, and V. Galitski, *Nat. Phys.* **7**, 490 (2011).
- [9] J.-i. Inoue and A. Tanaka, *Phys. Rev. Lett.* **105**, 017401 (2010).
- [10] M. Ezawa, *Phys. Rev. Lett.* **110**, 026603 (2013).
- [11] P. Delplace, A. Gómez-León, and G. Platero, *Phys. Rev. B* **88**, 245422 (2013).
- [12] T. Kitagawa, E. Berg, M. Rudner, and E. Demler, *Phys. Rev. B* **82**, 235114 (2010).
- [13] M. S. Rudner, N. H. Lindner, E. Berg, and M. Levin, *Phys. Rev. X* **3**, 031005 (2013).
- [14] P. Titum, E. Berg, M. S. Rudner, G. Refael, and N. H. Lindner, *Phys. Rev. X* **6**, 021013 (2016).
- [15] Y. Wang, H. Steinberg, P. Jarillo-Herrero, and N. Gedik, *Science* **342**, 453 (2013).
- [16] F. Mahmood, C.-K. Chan, Z. Alpichshev, D. Gardner, Y. Lee, P. A. Lee, and N. Gedik, *Nat. Phys.* **12**, 306 (2016).
- [17] D. Fausti, R. Tobey, N. Dean, S. Kaiser, A. Dienst, M. C. Hoffmann, S. Pyon, T. Takayama, H. Takagi, and A. Cavalleri, *Science* **331**, 189 (2011).

- [18] R. Mankowsky, A. Subedi, M. Först, S. Mariager, M. Chollet, H. Lemke, J. Robinson, J. Glownia, M. Minitti, A. Frano *et al.*, *Nature* **516**, 71 (2014).
- [19] M. Mitrano, A. Cantaluppi, D. Nicoletti, S. Kaiser, A. Perucchi, S. Lupi, P. Di Pietro, D. Pontiroli, M. Riccò, S. R. Clark *et al.*, *Nature* **530**, 461 (2016).
- [20] M. Knap, M. Babadi, G. Refael, I. Martin, and E. Demler, *Phys. Rev. B* **94**, 214504 (2016).
- [21] M. Babadi, M. Knap, I. Martin, G. Refael, and E. Demler, *Phys. Rev. B* **96**, 014512 (2017).
- [22] A. Singer, S. K. K. Patel, R. Kukreja, V. Uhlř, J. Wingert, S. Festersen, D. Zhu, J. M. Glownia, H. T. Lemke, S. Nelson *et al.*, *Phys. Rev. Lett.* **117**, 056401 (2016).
- [23] K. W. Kim, A. Pashkin, H. Schäfer, M. Beyer, M. Porer, T. Wolf, C. Bernhard, J. Demsar, R. Huber, and A. Leitenstorfer, *Nat. Mater.* **11**, 497 (2012).
- [24] J. Mentink, K. Balzer, and M. Eckstein, *Nat. Commun.* **6**, 6708 (2015).
- [25] K. Takasan, M. Nakagawa, and N. Kawakami, *Phys. Rev. B* **96**, 115120 (2017).
- [26] M. Claassen, H.-C. Jiang, B. Moritz, and T. P. Devereaux, *Nature Comm.* **8**, 1192 (2017).
- [27] A. G. Grushin, Á. Gómez-León, and T. Neupert, *Phys. Rev. Lett.* **112**, 156801 (2014).
- [28] Á. Rapp, X. Deng, and L. Santos, *Phys. Rev. Lett.* **109**, 203005 (2012).
- [29] J. Gong, L. Morales-Molina, and P. Hänggi, *Phys. Rev. Lett.* **103**, 133002 (2009).
- [30] L. W. Clark, L.-C. Ha, C.-Y. Xu, and C. Chin, *Phys. Rev. Lett.* **115**, 155301 (2015).
- [31] L. D'Alessio and M. Rigol, *Phys. Rev. X* **4**, 041048 (2014).
- [32] A. Lazarides, A. Das, and R. Moessner, *Phys. Rev. E* **90**, 012110 (2014).
- [33] D. A. Abanin, W. De Roeck, and F. Huveneers, *Phys. Rev. Lett.* **115**, 256803 (2015).
- [34] D. Abanin, W. De Roeck, W. W. Ho, and F. Huveneers, *Commun. Math. Phys.* **354**, 809 (2017).
- [35] T. Kuwahara, T. Mori, and K. Saito, *Ann. Phys.* **367**, 96 (2016).
- [36] F. Machado, G. D. Meyer, D. V. Else, C. Nayak, and N. Y. Yao, [arXiv:1708.01620](https://arxiv.org/abs/1708.01620).
- [37] M. Bukov, M. Kolodrubetz, and A. Polkovnikov, *Phys. Rev. Lett.* **116**, 125301 (2016).
- [38] W. F. Brinkman and T. M. Rice, *Phys. Rev. B* **2**, 1324 (1970).
- [39] C. L. Kane, P. A. Lee, and N. Read, *Phys. Rev. B* **39**, 6880 (1989).
- [40] K. I. Kugel' and D. Khomskii, *Phys. Usp.* **25**, 231 (1982).
- [41] Y. Tokura and N. Nagaosa, *Science* **288**, 462 (2000).
- [42] A. Georges, L. de' Medici, and J. Mravlje, *Annu. Rev. Condens. Matter Phys.* **4**, 137 (2013).
- [43] J. Liu, K. Hejazi, and L. Balents, *Phys. Rev. Lett.* **121**, 107201 (2018).
- [44] P. Fazekas, *Lecture Notes on Electron Correlation and Magnetism*, Vol. 5 (World Scientific, Singapore, 1999).
- [45] R. Sensarma, D. Pekker, M. D. Lukin, and E. Demler, *Phys. Rev. Lett.* **103**, 035303 (2009).
- [46] Since here we are dealing with frequencies that are very smaller than the energy scales of the model, it would be legitimate to use  $\tilde{T}(t=0)$  in equations defining the Green's functions, such as (10) and (14). This means that the hopping operators used in defining Green's functions are essentially the static ones.
- [47] J. Kanamori, *Prog. Theor. Phys.* **30**, 275 (1963).
- [48] E. Pavarini, S. Biermann, A. Poteryaev, A. I. Lichtenstein, A. Georges, and O. K. Andersen, *Phys. Rev. Lett.* **92**, 176403 (2004).
- [49] K. I. Kugel and D. I. Khomskii, *Zh. Eksp. Teor. Fiz* **64**, 1429 (1973).
- [50] DLMF, NIST Digital Library of Mathematical Functions, <http://dlmf.nist.gov/>, Release 1.0.17 of 2017-12-22, f. W. J. Olver, A. B. Olde Daalhuis, D. W. Lozier, B. I. Schneider, R. F. Boisvert, C. W. Clark, B. R. Miller and B. V. Saunders (eds.), URL <http://dlmf.nist.gov/>.
- [51] N. M. Temme, *Numer. Algor.* **15**, 207 (1997).